

See discussions, stats, and author profiles for this publication at: <https://www.researchgate.net/publication/215612963>

Intermolecular Interactions from a Natural Bond Orbital, Donor–Acceptor Viewpoint

ARTICLE *in* CHEMICAL REVIEWS · SEPTEMBER 1988

Impact Factor: 46.57 · DOI: 10.1021/cr00088a005

CITATIONS

9,423

READS

981

3 AUTHORS, INCLUDING:



[Frank Weinhold](#)

University of Wisconsin–Madison

199 PUBLICATIONS 28,089 CITATIONS

[SEE PROFILE](#)

Intermolecular Interactions from a Natural Bond Orbital, Donor–Acceptor Viewpoint

ALAN E. REED*

Institut für Organische Chemie der Universität Erlangen-Nürnberg, Henkestrasse 42, 8520 Erlangen, Federal Republic of Germany

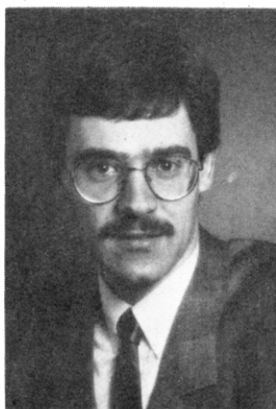
LARRY A. CURTISS*

Chemical Technology Division/Materials Science and Technology Program, Argonne National Laboratory, Argonne, Illinois 60439

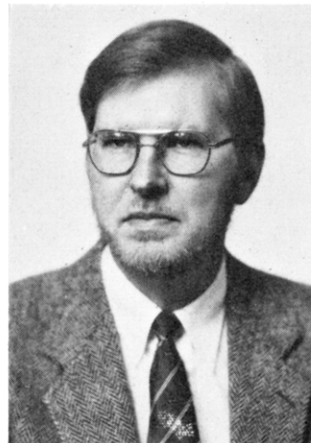
FRANK WEINHOLD*

*Theoretical Chemistry Institute and Department of Chemistry, University of Wisconsin, Madison, Wisconsin 53706**Received November 10, 1987 (Revised Manuscript Received February 16, 1988)***Contents**

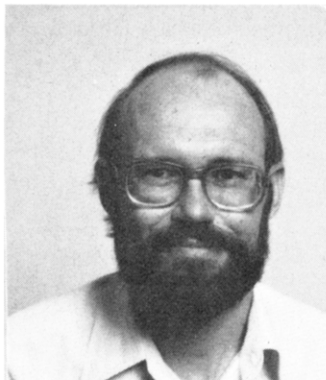
I. Introduction	899	D. Chemisorption	917
II. Natural Bond Orbital Analysis	902	E. Relationships between Inter- and Intramolecular Interactions	918
A. Occupancy-Weighted Symmetric Orthogonalization	902	IV. Relationship of Donor–Acceptor and Electrostatic Models	919
B. Natural Orbitals and the One-Particle Density Matrix	903	A. Historical Overview	919
C. Atomic Eigenvectors: Natural Atomic Orbitals and Natural Population Analysis	904	B. Relationship to Kitaura–Morokuma Analysis	920
D. Bond Eigenvectors: Natural Hybrids and Natural Bond Orbitals	904	C. Semiempirical Potential Functions	921
E. Natural Localized Molecular Orbitals	905	V. Concluding Remarks	922
F. Hyperconjugative Interactions in NBO Analysis	906		
III. Intermolecular Donor–Acceptor Models Based on NBO Analysis	906		
A. H-Bonded Neutral Complexes	906	I. Introduction	
1. Water Dimer	906	The past 15 years has witnessed a golden age of discovery in the realm of “van der Waals chemistry”. The van der Waals bonding regime lies at the interface between two well-studied interaction types: the short-range, strong (chemical) interactions of covalent type, and the long-range, weak (physical) interactions of dispersion and multipole type. It was therefore surprising to discover that this borderline region gives rise to species whose structural and energetic patterns are distinctively novel. As experimental nozzle beam ^{1–4} and ab initio computational studies ^{5,6} have combined to reveal the rich architectural patterns of van der Waals bonding, efforts have been made to extend the elementary principles of valence theory to encompass such bonds within a general conceptual framework of covalent and noncovalent interactions. The present article reviews progress that has been made toward this goal by the method of natural bond orbital analysis, particularly for H-bonded and other strongly bound van der Waals complexes.	
2. OC···HF and CO···HF	908	Natural bond orbital (NBO) analysis originated ⁷ as a technique for studying hybridization and covalency effects in polyatomic wave functions, based on local block eigenvectors of the one-particle density matrix (see section II). NBOs were conceived as a “chemist’s basis set” that would correspond closely to the picture of localized bonds and lone pairs as basic units of molecular structure. The NBO for a localized σ bond σ_{AB} between atoms A and B is formed from directed or	
3. Complexes of NO and HF	909		
4. Survey of a Large Series of H-Bond Complexes	910		
5. Cooperativity in H-Bonding	911		
6. Hydrophobic Interactions	912		
7. Other Topics	913		
B. Non-H-Bonded Neutral Complexes	914		
1. Survey of a Large Series of Non-H-Bonded Complexes	914		
2. Competition between H-Bonded and Non-H-Bonded Structures	914		
3. Complexes of Rare Gases with BeO	915		
C. Ion–Molecule Complexes and Contact Ion Pairs	915		
1. Anion–Water Complexes	915		
2. Cation–Water Complexes	916		
3. Bifluoride Ion	916		
4. “Salt” Isomer of Carbon Tetrachloride	916		
5. Ground and Excited States of $(CO)_2^+$	916		



Alan E. Reed was born in Chicago, IL, in 1958 and received his B.S. degree in chemistry from the University of Illinois at Champaign-Urbana in 1980, having carried out experimental research both there and at the University of Chicago. He received his Ph.D. in physical chemistry from the University of Wisconsin at Madison in 1985, working with Prof. Frank Weinhold, a part of this work being carried out with Dr. Larry Curtiss at Argonne National Laboratory. Currently, he is doing postdoctoral research with Prof. Paul von Ragué Schleyer at Erlangen, West Germany. His scientific interests concern the rich range of diversity and possibility in chemical structure and bonding, from solid state to biochemical systems, and have focused primarily on the theoretical description of inter- and intramolecular bonding involving elements H to Ar, including studies of hypervalency, hyperconjugation, and the anomeric effect.



Frank A. Weinhold was born in Scottsbluff, NB, in 1941. He studied chemistry as an undergraduate at the University of Colorado, Boulder (1958–1962), as a Fulbright Scholar at the Universität Freiburg/Breisgau in Germany (1962–1963), and as a graduate student (under Prof. E. B. Wilson, Jr.) at Harvard University, where he received the Ph.D. degree in physical chemistry in 1967. His postdoctoral studies were at Oxford (with Prof. C. A. Coulson) and Berkeley (Miller Fellow). He has taught at Stanford University and the University of Wisconsin, Madison, where he is currently Professor of Chemistry and Director of the Theoretical Chemistry Institute. His principal research interests include upper and lower bounds for quantum mechanical properties, metric geometry of equilibrium thermodynamics, and natural bond orbital studies of covalent and noncovalent interactions.



Larry A. Curtiss was born in Madison, WI, in 1947 and received his B.S. degree in chemistry from the University of Wisconsin in 1969. He received his Ph.D. degree in physical chemistry in 1973 working with Professor John A. Pople. He then spent about 2 years as a Battelle Institute Fellow at Battelle Memorial Institute (working with Professor C. W. Kern) in Columbus, OH. In 1976 he joined the Chemical Technology Division at Argonne National Laboratory. His research interests include theoretical studies of van der Waals complexes, ordered and ionic solutions, zeolites, heterogeneous charge-transfer reactions, and small molecules and their cations. In addition, he has been involved in experimental studies of gas-phase association reactions.

thonormal hybrids h_A , h_B [natural hybrid orbitals (NHOs)]

$$\sigma_{AB} = c_A h_A + c_B h_B \quad (1a)$$

and the natural hybrids in turn are composed from a set of effective valence-shell atomic orbitals [natural atomic orbitals (NAOs)],^{8,9} optimized for the chosen wave function. A distinguishing feature of such natural localized functions (analogous to classic "natural orbitals" in the Löwdin delocalized sense¹⁰) is the simultaneous requirement of *orthonormality* and *maximum occupancy*, leading to compact expressions for

atomic and bond properties. Ab initio wave functions transformed to NBO form are found to be in good agreement with Lewis structure concepts and with the basic Pauling-Slater-Coulson picture¹¹ of bond hybridization and polarization. The filled NBOs σ_{AB} of the "natural Lewis structure" are therefore well adapted to describing covalency effects in molecules.

However, the general transformation to NBOs also leads to orbitals that are unoccupied in the formal Lewis structure and that may thus be used to describe noncovalency effects. The most important of these are the antibonds σ^*_{AB} ¹²

$$\sigma^*_{AB} = c_B h_A - c_A h_B \quad (1b)$$

which arise from the same set of atomic valence-shell hybrids that unite to form the bond functions σ_{AB} , eq 1a. The antibonds represent unused valence-shell capacity, spanning portions of the atomic valence space that are formally unsaturated by covalent bond formation. Small occupancies of these antibonds correspond, in Hartree-Fock theory, to irreducible departures from the idealized Lewis picture and thus to small noncovalent corrections to the picture of localized covalent bonds.

The energy associated with the antibonds can be numerically assessed by *deleting* these orbitals from the basis set and recalculating the total energy to determine the associated variational energy lowering. In this way one obtains a decomposition of the total energy E into components associated with covalent ($E_{\sigma\sigma} = E_{\text{Lewis}}$) and noncovalent ($E_{\sigma\sigma^*} = E_{\text{non-Lewis}}$) contributions

$$E = E_{\sigma\sigma} + E_{\sigma\sigma^*} \quad (2)$$

NBO decompositions of this form have now been obtained for a large number of closed-shell and open-shell¹³ molecular species. In equations such as (1) and

TABLE I. NBO Energy Decompositions for Selected Molecules (RHF/6-31G* Level, Pople-Gordon Idealized Geometry), Showing the Covalent Contribution $E(\text{Lewis}) = E_{\sigma\sigma}$, the Noncovalent Contribution $E(\text{non-Lewis}) = E_{\sigma\sigma^*}$, and the Percentage Contribution % $E(\text{Lewis})$ Associated with the Natural Lewis Structure^a

molecule	$E(\text{Lewis})$	$E(\text{non-Lewis})$	% $E(\text{Lewis})$
BH ₃	-26.384470	-0.005434	99.979
CH ₄	-40.187329	-0.007732	99.981
NH ₃	-56.180217	-0.003527	99.994
H ₂ O	-76.007041	-0.002827	99.996
HF	-100.001908	-0.000900	99.999
AlH ₃	-243.570589	-0.045162	99.982
SiH ₄	-291.192327	-0.032763	99.989
PH ₃	-342.410798	-0.019140	99.994
H ₂ S	-398.652368	-0.007483	99.998
HCl	-460.056952	-0.002661	99.999
CF ₃ H	-336.469129	-0.295778	99.912
C ₂ H ₆	-79.170183	-0.057562	99.927
C ₂ H ₄	-77.953649	-0.076717	99.902
C ₂ H ₂	-76.728306	-0.089021	99.884
H ₂ CO	-118.762634	-0.101071	99.911
C ₆ H ₆	-230.107441	-0.594436	99.742

^a Note the effect of vicinal $\sigma \rightarrow \sigma^*$ interactions (molecules 11–15 of the list) and of aromatic “resonance” (C_6H_6) in reducing the dominance of a single Lewis structure.

(2), the symbols “ σ ” and “ σ^* ” will be used in a generic sense to refer to filled and unfilled orbitals of the formal Lewis structure, though the former orbitals may actually be core orbitals (c), lone pairs (n), σ or π bonds (σ , π), etc., and the latter may be σ or π antibonds (σ^*, π^*), extra-valence-shell Rydberg (r) orbitals, etc., according to the specific case.

In the NBO decomposition (2), the noncovalent contributions $E_{\sigma\sigma^*}$ are typically much less than 1% of the contribution of $E_{\sigma\sigma}$, reflecting the dominance of the Lewis-type component of the bonding. Table I demonstrates the accuracy of this Lewis-type description of the wave function for a variety of first- and second-row hydrides and simple organic molecules at the ab initio RHF/6-31G* level.¹⁴ As can be seen in this table, the corrections to the Lewis-type picture are usually so small as to be well approximated by simple second-order perturbative expressions of the type illustrated in Figure 1. This figure depicts the interaction of a filled orbital σ of the formal Lewis structure with one of the unfilled antibonding orbitals σ^* to give the second-order energy lowering, $\Delta E_{\sigma\sigma^*}^{(2)}$. In SCF-MO theory (to which attention is primarily restricted in this review),¹⁵ this energy lowering is given by the formula

$$\Delta E_{\sigma\sigma^*}^{(2)} = -2 \frac{\langle \sigma | \hat{F} | \sigma^* \rangle^2}{\epsilon_{\sigma^*} - \epsilon_\sigma} \quad (3)$$

where \hat{F} is the Fock operator and ϵ_σ and ϵ_{σ^*} are NBO orbital energies. The NBO perturbative framework permits one to apply qualitative concepts of valence theory to describe the noncovalent energy lowerings (3). For example, the strengths of the perturbative Fock matrix elements can be related to the shapes of the bond and antibond orbitals through the NBO counterpart of the Mulliken approximation, allowing the noncovalent energy lowerings to be described in terms of a generalized “principle of maximum overlap” between bonds and antibonds.

The antibonding NBOs { σ^*_{AB} } must not be confused with the virtual MOs of SCF-MO theory. The virtual

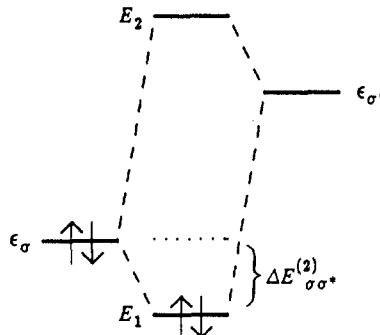


Figure 1. Perturbative donor–acceptor interaction, involving a filled orbital σ and an unfilled orbital σ^* .

MOs are strictly unoccupied and thus play no role in the wave function or any observable property, whereas the antibonds { σ^*_{AB} } generally exhibit nonzero occupancies, and their contributions lead to definite energy lowerings and changes in the form of the wave function. The role of antibonds can be seen by transforming the occupied canonical MOs to *localized* molecular orbital (LMO)¹⁶ form (section II.E). The LMO ϕ_{AB}^{LMO} associated with a localized A–B bond may be written in NBO form as

$$\phi_{AB}^{LMO} \simeq \sigma_{AB} + \lambda \sigma^*_{CD} + \dots \quad (4)$$

where the small contribution of the antibond σ^*_{CD} represents the irreducible delocalization of σ_{AB} from an idealized localized form, due to hyperconjugative noncovalent interactions. Only in the idealized limit of a strictly localized Lewis structure would the antibonds lie entirely in the virtual MO space.

Since the noncovalent delocalization effects (3) and (4) [cf. Figure 1] are associated with $\sigma \rightarrow \sigma^*$ interactions between filled (donor) and unfilled (acceptor) orbitals, it is natural to describe them as being of “donor–acceptor”, “charge transfer”, or generalized “Lewis base–Lewis acid” type. Such terms should not be confused with HOMO–LUMO interactions,¹⁷ as explained above, nor should they be confused with “ionic resonance” of the sort associated with Mulliken’s classic treatment of charge-transfer complexes,¹⁸ since the quantity of charge q transferred

$$q \simeq 2|\lambda|^2 \simeq |\Delta E_{\sigma\sigma^*}^{(2)}| / \epsilon_{\sigma^*} - \epsilon_\sigma \quad (5)$$

($\sim 10^{-3}$ e) is typically much less than that required for formation of an ion pair.

The present work is chiefly concerned with intermolecular donor–acceptor interactions, arising from the noncovalent term $E_{\sigma\sigma^*}$ of eq 2. However, it is important to recognize that the covalent term $E_{\sigma\sigma}$ also contributes to intermolecular forces. The idealized natural Lewis structure commonly accounts for >99% of the total electron density (cf. section IID) and so includes the preponderant portion of the exchange and electrostatic multipole effects associated with the monomer charge distributions. Furthermore, as monomer separation varies, the charge distributions can readjust in response to their mutual polarizing effects; such polarization contributions are also reflected in the form of the occupied NBOs and the interaction term $E_{\sigma\sigma}$. Indeed, in the long-range limit where exchange effects are negligible, the intermolecular interaction arises only from the term $E_{\sigma\sigma}$, since the integrals contributing to this

term typically have a weaker (multipole) fall-off with distance than do the exponential terms contained in $E_{\sigma\sigma^*}$. Nevertheless, at the actual equilibrium separation of many strong van der Waals complexes, the term $E_{\sigma\sigma^*}$ is found to be far the more significant contribution to the bonding, as discussed in section III.

Since the NBO decompositions (1) and (2) can be carried out for very general wavefunctions (up to and including the true wave function), they are consistent with full quantum mechanical treatment of the van der Waals complex (including exact satisfaction of the Pauli principle) at all separations. Although the NBO energy term $E_{\sigma\sigma}$ reduces properly to a classical electrostatic limit in the long-range asymptotic regime, it is found that such a reduction is not numerically valid at the actual separations of strongly bound van der Waals complexes (particularly, H-bonded species), which are often significantly inside the distance of contact of empirical van der Waals radii. NBO analysis therefore emphasizes the importance of *quantum mechanical orbital interaction and exchange effects* in the van der Waals regime, distinguishable from classical electrostatic effects. The relationship to models derived by assuming the applicability of classical electrostatic formulas in the van der Waals bonding region is discussed in sections III and IV.

NBO analysis also differs from earlier methods of wave function analysis that employ alternative criteria to define filled and unfilled orbitals or that allow overlap of these orbitals. The strict orthogonality of NBOs is particularly important with respect to a physically meaningful perturbative analysis of the wave function (as explained in section II.A). In section IV we analyze how changes in the treatment of orthogonality, particularly those corresponding to an unbalanced treatment of atomic valence subspaces, can lead to dramatic changes in the perceived origin of H-bonding and other strong forms of van der Waals complexation. Generally speaking, NBO analysis allows one to isolate H-bond interaction energies in low-order perturbative expressions of easily interpreted form and to relate these expressions to chemical explanations of H-bonding based on orbital interaction concepts. The results of NBO analysis are often in surprisingly close agreement with qualitative concepts that preceded the era of large-scale computations. NBO analysis has thus tended to differ from other methods of analysis in suggesting how modern ab initio wave functions can be brought into essential harmony with earlier qualitative viewpoints.

The general plan of this review is as follows. Section II describes the mathematical methodology of NBO analysis, including outlines of the algorithms for natural atomic orbitals, natural population analysis, natural hybrid and bond orbitals, and natural localized molecular orbitals. Section III surveys recent applications of NBO analysis to a large number of chemical systems, including studies of various H-bonded and non-H-bonded neutral and ionic complexes, rare-gas complexes with BeO, hydrophobic interactions, cooperativity effects, chemisorption, etc., and relationships to associated intramolecular interactions. Section IV presents a detailed comparison of the NBO donor-acceptor model with the more conventional electrostatic models of van der Waals bonding, focusing on relationships to analysis methods of Kitaura-Morokuma type. Section

V presents concluding remarks concerning the limits of the donor-acceptor picture and some future prospects in van der Waals chemistry.

II. Natural Bond Orbital Analysis

Natural bond orbital analysis comprises a sequence of transformations from the input basis set $\{\chi_i\}$ to various localized basis sets [natural atomic orbitals (NAOs), hybrid orbitals (NHOs), bond orbitals (NBOs), and localized molecular orbitals (NLMOs)]

$$\text{input basis} \rightarrow \text{NAOs} \rightarrow \text{NHOs} \rightarrow \text{NBOs} \rightarrow \text{NLMOs} \quad (6)$$

The localized sets may be subsequently transformed to delocalized natural orbitals (NOs) or canonical molecular orbitals (MOs). These steps are automated by the NBO computer program,¹⁹ which has been attached to a variety of ab initio and semiempirical electronic structure packages (GAUSSIAN-82, GAMESS, MOPAC, AMPAC, etc.).²⁰ Each step of the sequence (6) involves an orthonormal set that spans the full space of the input basis set and can be used to give an exact representation of the calculated wave function and operators (properties) of the system. In this section we outline some general characteristics of the transformations (6) and the specifics of individual steps.

A. Occupancy-Weighted Symmetric Orthogonalization

The method of constructing NAOs and NBOs rests in an essential way on the occupancy-weighted symmetric orthogonalization procedure,^{8,9} which is imposed at the *atomic orbital* stage in the formation of NAOs from the chosen basis AOs. The subsequent formation of natural hybrids (NHOs) and bond orbitals (NBOs) involves unitary transformations similar to those envisioned in elementary bonding discussions [cf. (1a,b)], so that orthogonality is automatically maintained. In semiempirical SCF-MO theory^{7,21} the basis AOs are generally taken to be implicitly orthogonal, and no special NAO transformation is required in this case.

Why are we concerned that atomic orbitals be mutually orthogonal? Löwdin was the first to clearly point out the "orthogonality dilemma"²² and the essential simplifications that result if AOs are orthogonalized. The mathematical and physical anomalies associated with nonorthogonal orbitals were recently analyzed in considerable detail.²³ It has been recognized that non-orthogonal AOs lead to non-Hermitian terms in the second-quantized form of the Hamiltonian, since field operators for nonorthogonal AOs do not satisfy proper Fermi-Dirac commutation relations.²⁴ The difficulties are particularly severe if the AOs are employed in perturbative-style "explanations", based on a "noninteracting" unperturbed Hamiltonian having these orbitals as eigenfunctions. Since a Hermitian Hamiltonian necessarily has orthogonal eigenfunctions,²⁵ the use of nonorthogonal AOs in a perturbative framework²⁶ necessarily implies use of a *non*-Hermitian (physically unrealizable) reference system, leading to nonconservation of probability densities, possible complex energies or transition probabilities, or related mathematical and physical inconsistencies. The assumption of or-

thogonality for the underlying AOs of elementary valence theory is therefore an *essential* prerequisite for the physical and mathematical consistency of perturbation-style analyses of chemical phenomena. Correspondingly, comparisons of ab initio wave functions with qualitative valence AO concepts can only be expected to have validity when the AOs are required to be orthonormal. As compared with nonorthogonal AOs, it has been shown that NAOs better satisfy the assumptions (zero differential overlap approximation, effective *minimal* basis set, etc.) associated with semiempirical valence theories.²³ Thus, NAOs better serve as the ab initio counterpart of the effective valence-shell AOs that underlie these theories.

In the NAO procedure, nonorthogonal AOs $\{\tilde{\phi}_i\}$ are transformed to corresponding orthonormal AOs $\{\phi_i\}$ by the occupancy-weighted symmetric orthogonalization (OWSO) procedure^{8,9}

$$\mathbf{T}_{\text{ows}} \{\tilde{\phi}_i\} = \{\phi_i\}, \quad \langle \phi_i | \phi_j \rangle = \delta_{ij} \quad (7a)$$

The transformation matrix \mathbf{T}_{ows} has the mathematical property of *minimizing* the occupancy-weighted, mean-squared deviations of the ϕ_i from the parent non-orthogonal $\tilde{\phi}_i$

$$\min \left\{ \sum_i w_i \int |\phi_i - \tilde{\phi}_i|^2 d\tau \right\} \quad (7b)$$

with weighting factor w_i :

$$w_i = \langle \tilde{\phi}_i | \hat{\Gamma} | \tilde{\phi}_i \rangle \quad (7c)$$

taken as the occupancy of $\tilde{\phi}_i$ (diagonal expectation value of the density operator $\hat{\Gamma}$). [The explicit form of \mathbf{T}_{ows} is obtained as a special case of the Carlson-Keller theorem²⁷ and is given in ref 9.] Property (7b) is a generalization of the maximum-resemblance property for the familiar Löwdin symmetric orthogonalization,²² which corresponds to choosing $w_i = 1$ for each i . In the OWSO procedure, those orbitals having highest occupancy are most strongly preserved in form, while orbitals of negligible occupancy can distort freely to achieve orthogonality. This property ensures numerical stability and convergence of the procedure as the basis set is extended to completeness.^{9,13}

For small, near-minimal basis sets, the OWSO and Löwdin symmetric orthogonalization (SO) procedures lead to similar orbitals. In this case, setting the weighting factors (7c) to unity removes the dependence on $\hat{\Gamma}$ and makes the orthogonalization transformation purely dependent on geometrical factors (elements of the overlap matrix \mathbf{S})

$$\mathbf{T}_{\text{ows}} \simeq \mathbf{T}_{\text{so}} = \mathbf{S}^{-1/2} \quad (8)$$

thereby simplifying the mathematical treatment. However, in extended basis sets the difference between \mathbf{T}_{so} and \mathbf{T}_{ows} becomes progressively greater,⁹ and the critical role of the occupancy weighting in ensuring smooth convergence toward a unique set of high-occupancy AOs becomes more important. We refer to the small set of high-occupancy (core plus valence shell) NAOs as the "natural minimal basis" (NMB) set. The NMB set is found to describe virtually all the electron density of the system, as simple valence-shell MO theory would suggest. Table II documents the accuracy of the minimal NMB description for a variety of first- and second-row molecules, showing the high percentage

TABLE II. NBO Decomposition of Total Electron Density for Selected Molecules (RHF/6-31G* Level, Pople-Gordon Idealized Geometry), Showing the Percentage Associated with the Natural Minimal Basis (NMB) NAOs [% $\rho(\text{NMB})$] and the Percentage Associated with the Optimal "Natural Lewis Structure" [% $\rho(\text{Lewis})$]

molecule	% $\rho(\text{NMB})$	% $\rho(\text{Lewis})$
BH ₃	99.89	99.95
CH ₄	99.91	99.97
NH ₃	99.82	99.98
H ₂ O	99.85	99.98
HF	99.91	99.99
AlH ₃	99.80	99.64
SiH ₄	99.72	99.81
PH ₃	99.57	99.90
H ₂ S	99.71	99.98
HCl	99.88	100.00
CF ₃ H	99.76	99.18
C ₂ H ₆	99.84	99.74
C ₃ H ₈	99.72	99.70
C ₂ H ₂	99.82	99.75
H ₂ CO	99.61	99.42
C ₆ H ₆	99.69	97.12

of the total electron density that can be associated with this subset of NAOs.

B. Natural Orbitals and the One-Particle Density Matrix

"Natural" orbitals in the classic Löwdin sense¹⁰ derive from properties of the one-particle density operator $\hat{\Gamma}(1|1')$

$$\hat{\Gamma}(1|1') = N \int \psi(1, 2, \dots, N) \psi^*(1', 2, \dots, N) d\tau_2 \dots d\tau_N \quad (9)$$

and its associated matrix representation Γ in an AO basis $\{\chi_i\}$

$$(\Gamma)_{ij} = \int \chi_i^*(1) \hat{\Gamma}(1|1') \chi_j(1') d\tau_1 d\tau_{1'} \quad (10)$$

By definition, the natural orbitals $\{\phi_i\}$ are the eigenorbitals of $\hat{\Gamma}$

$$\hat{\Gamma} \phi_i = \gamma_i \phi_i \quad (11)$$

with corresponding eigenvalues (occupation numbers) γ_i . As shown originally by Löwdin, the natural orbitals have an important *optimum* property that leads to the most rapidly convergent expansion of the electron density $\rho(r) = \hat{\Gamma}(r|r)$. If we seek an approximation to $\rho(r)$ using a finite orthonormal basis set $\{\chi_k\}$ of n orbitals, with positive weighting coefficients w_k

$$\rho(r) \simeq \sum_{k=1}^n w_k |\chi_k(r)|^2 \quad (12)$$

then, for each $n = 1, 2, \dots$, the *best possible* representation of $\rho(r)$ in the mean-squared sense is achieved by choosing $\chi_i = \phi_i$ and $w_i = \gamma_i$ in order, $i = 1, 2, \dots, n$. This maximum-occupancy property gives rise to the extremely compact representations of electron density and other one-electron properties that distinguish natural orbitals from other basis sets.

In open-shell systems, the density operator separates into distinct components for α and β spin, leading to the possibility of different NBOs for different spins.¹³ In closed-shell systems, to which attention is primarily restricted here, the spatial parts of these operators are identical, and the operator of interest is the spinless

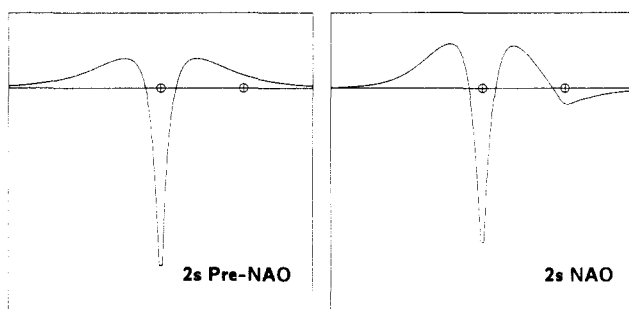


Figure 2. Carbon atom 2s pre-NAO (left) and NAO (right) in methane (RHF/6-31G* level), showing the additional NAO nodal feature that is present in the region of the adjacent hydrogen nucleus.

density operator obtained by summing over the two spin components. Open-shell NBOs are discussed briefly in sections III.A.3, III.C.5, and III.D.

C. Atomic Eigenvectors: Natural Atomic Orbitals and Natural Population Analysis

Localized natural orbitals are obtained as eigenvectors of localized *blocks* of the density matrix. The localized eigenvectors satisfy maximum-occupancy properties analogous to those described above, eq 12, for representing the electron density associated with that block.

For example, atomic (one-center) eigenvectors $\phi_i^{(A)}$ on atom A are obtained by diagonalizing the localized block $\Gamma^{(A)}$ of the full density matrix Γ , associated with basis functions $\chi_i^{(A)}$ on that atom. Since the eigenvectors $\phi_i^{(A)}$ of each block are orthogonal among themselves, but not to eigenvectors $\phi_i^{(B)}$ from other blocks, the final NAOs are obtained by removing interatomic overlap by the OWSO procedure (7). In practice, each atomic block is first averaged over angular components (e.g., p_x , p_y , p_z) to preserve free-atom symmetries and guarantee overall rotational invariance.⁹

An interesting formal difficulty arises if the basis functions are not atom-centered, i.e., if single-center expansions, bond-centered functions, or James-Coolidge-type basis functions are employed. In this case, the initial partitioning of the density matrix into atomic blocks must be preceded by separate calculations (in the chosen basis set) of natural orbitals $\chi_i^{(A)}$ for each isolated atom A. A composite basis set of linearly independent atom-centered orbitals can then be assembled from the leading $\chi_i^{(A)}$'s of these separate atomic calculations, and the derivation of NAOs proceeds in the usual way. In practice, atom-centered basis sets are generally employed,¹⁴ so that the partitioning of Γ is straightforward.

It is useful to distinguish the NAOs $\phi_i^{(A)}$ from the associated "pre-NAOs" $\tilde{\phi}_i^{(A)}$, which differ only in the omission of the final interatomic orthogonalization step. The pre-NAOs lack the "orthogonalization tails" at the positions of other nuclei, so their shapes more nearly resemble familiar hydrogenic or Hartree-Fock orbitals of isolated atoms. Figure 2 compares diagrams of the carbon 2s NAO (ϕ_{2s}) and pre-NAO ($\tilde{\phi}_{2s}$) of methane (RHF/6-31G* level) to illustrate the difference. The utility of pre-NAOs is to provide estimates of NAO Fock matrix elements $\langle \phi_i^{(A)} | \hat{F} | \phi_j^{(B)} \rangle$ in terms of pre-NAO

overlap integrals $\langle \tilde{\phi}_i^{(A)} | \tilde{\phi}_j^{(B)} \rangle$ through Mulliken-type approximations²⁸ of the form

$$\langle \phi_i^{(A)} | \hat{F} | \phi_j^{(B)} \rangle \simeq k \langle \tilde{\phi}_i^{(A)} | \tilde{\phi}_j^{(B)} \rangle \quad (13)$$

This allows one to retain the useful concept that interaction strength is proportional to overlap and to use the *shapes* of the pre-NAOs to estimate the radial and angular dependence of Fock matrix elements such as those of eq 3. Reed and Schleyer²⁹ have recently studied the proportionality constants k for a variety of first- and second-row atoms.

The orthonormal NAOs $\{\phi_i^{(A)}\}$ provide the basis for an improved "natural population analysis"⁹ which corrects many of the deficiencies of the well-known Mulliken population analysis.³⁰ The natural population $q_i^{(A)}$ of orbital $\phi_i^{(A)}$ on atom A is simply the diagonal density matrix element in the NAO basis

$$q_i^{(A)} = \langle \phi_i^{(A)} | \hat{\Gamma} | \phi_i^{(A)} \rangle \quad (14)$$

These populations automatically satisfy the Pauli principle ($0 \leq q_i^{(A)} \leq 2$) and give atomic populations $q^{(A)}$ that sum properly to the total number of electrons

$$q^{(A)} = \sum_i q_i^{(A)}, \quad N_{\text{elec}} = \sum_A^{\text{atoms}} q^{(A)} \quad (15)$$

Natural population analysis has been applied to a wide variety of chemical systems³¹ and has been shown to exhibit good numerical stability and agreement with other theoretical and experimental measures of charge distribution. In the present context, its principal use is to assess the intermolecular charge transfer q (cf. eq 5) that accompanies formation of a van der Waals complex. In accordance with eq 5, one finds an approximate proportionality between the natural charge transfer q and the associated energy lowering ΔE [i.e., $q \propto \Delta E$, with a proportionality constant (in atomic units) of order unity], so that natural population changes of the order of 0.001 e correspond to chemically significant energy changes (0.001 au ≈ 0.6 kcal/mol).

D. Bond Eigenvectors: Natural Hybrids and Natural Bond Orbitals

With the density matrix transformed to the NAO basis, the NBO program¹⁹ begins the search for an optimal natural Lewis structure. NAOs of high occupancy (> 1.999 e) are removed as unhybridized core orbitals K_A . The program next loops over one-center blocks $\Gamma^{(A)}$, searching for lone-pair eigenvectors n_A whose occupancy exceeds a preset pair threshold ($\rho_{\text{thresh}} = 1.90$). The density matrix is depleted of eigenvectors satisfying this threshold, and the program then cycles over all two-center blocks $\Gamma^{(AB)}$ searching for bond vectors σ_{AB} whose occupancy exceeds ρ_{thresh} . (The search may be further extended to three-center bonds if an insufficient number of electron pairs were found in the one- and two-center searches.) Each σ_{AB} is decomposed into its normalized hybrid contributions h_A and h_B from each atom, eq 1a, and hybrids from each center participating in different bonds are symmetrically orthogonalized to remove intraatomic overlap. The set of localized electron pairs (K_A)²(n_A)²(σ_{AB})²... found in this way constitutes a "natural Lewis structure" to describe the system.

The accuracy of this Lewis structure may be assessed by the total occupancy ρ_{Lewis} of its occupied NBOs,

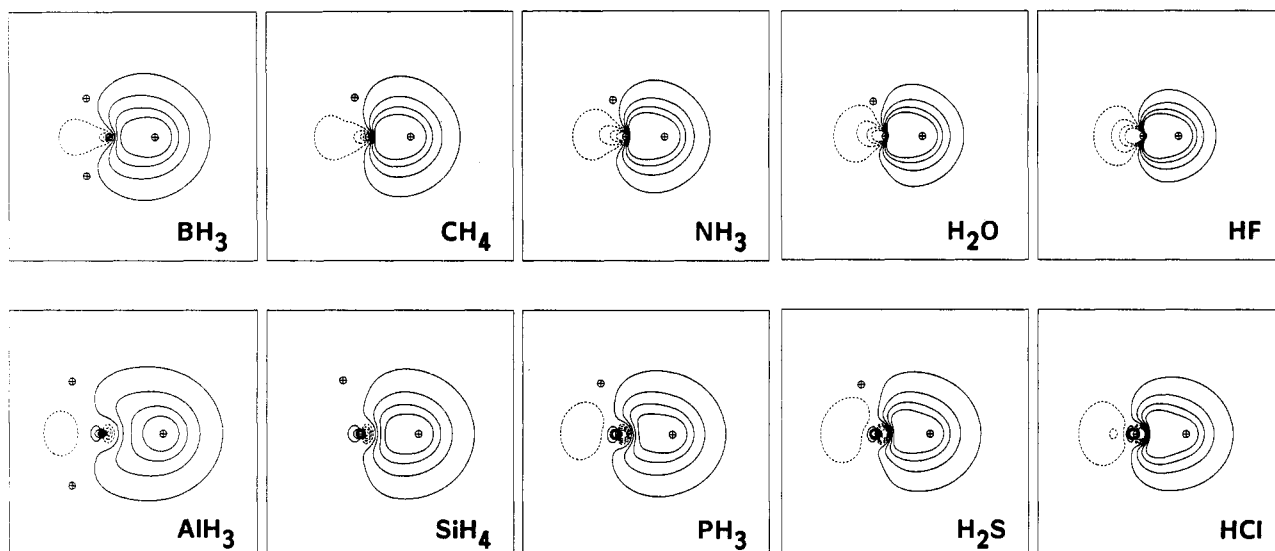
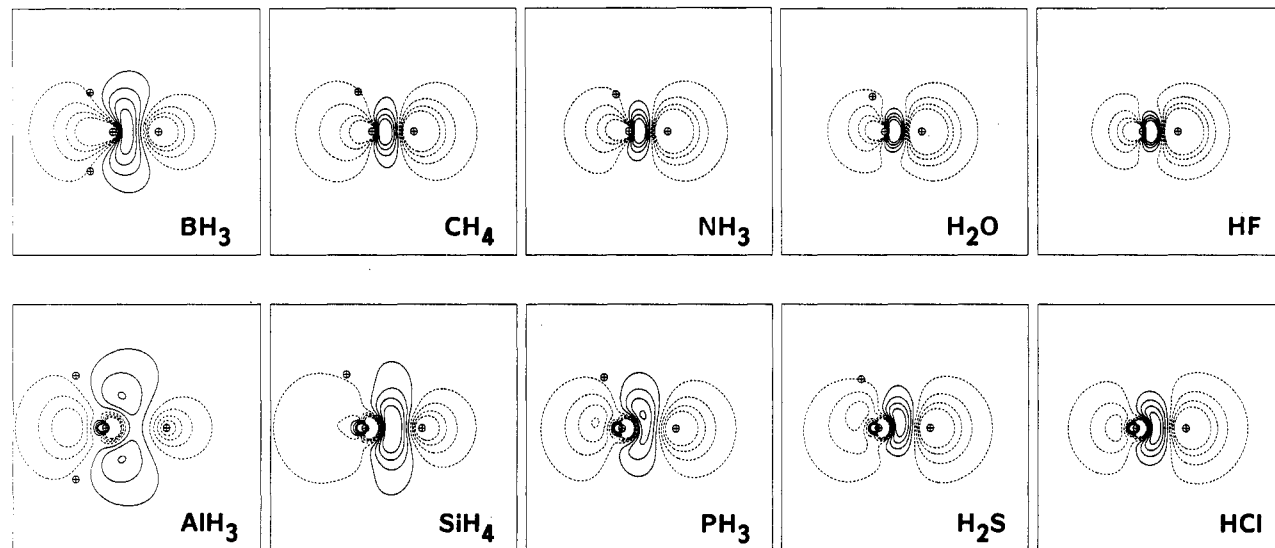
a. A-H Bond NBOs**b. A-H* Antibond NBOs**

Figure 3. Contour plots of first- and second-row hydride bonds σ_{AH} (a) and antibonds σ^*_{AH} (b), showing periodic trends in the polarization and diffuseness of the NBOs (RHF/6-31G* level, idealized Pople-Gordon geometry).

which is commonly found to exceed 99.9% of the total electron density for ordinary molecules. Table II summarizes the value of ρ_{Lewis} for a variety of first- and second-row hydrides and simple organic molecules to demonstrate the accuracy of the natural Lewis structure description. In the less usual ("resonance") case where the difference $\rho^* = \rho_{\text{total}} - \rho_{\text{Lewis}}$ exceeds one electron, or, when individual σ^* occupancies exceed 0.10, ρ_{thresh} is successively lowered (1.80, ..., 1.50) and the NBO search is repeated for each value. The best NBO Lewis structure is that corresponding to largest overall ρ_{Lewis} and is generally found to agree with the pattern of bonds and lone pairs of the chemist's standard structural Lewis formula. Figure 3 illustrates contour diagrams of σ_{AH} and σ^*_{AH} NBOs (RHF/6-31G* level) for some simple first- and second-row AH_n hydride molecules. These diagrams illustrate how the NBOs automatically incorporate systematic changes in bond hybridization and polarization, reflecting the expected

periodic trends associated with atomic electronegativity differences. These functions have been found to be highly transferable from one molecule to another³² and to correspond well with Bent's rule³³ and other empirical measures of bond hybridization.

E. Natural Localized Molecular Orbitals

In the NBO basis, the density matrix is partitioned into a block ($\Gamma_{\sigma\sigma}$) associated with the highly occupied NBOs of the natural Lewis structure and a block ($\Gamma_{\sigma^*\sigma^*}$) associated with the remaining weakly occupied NBOs of antibond and Rydberg type. The off-diagonal matrix elements connecting these blocks ($\Gamma_{\sigma\sigma^*}$) represent the irreducible $\sigma \rightarrow \sigma^*$ mixing of filled and unfilled orbitals which lead to partial breakdown of the strictly localized Lewis structure picture. By carrying out a succession of 2×2 Jacobi rotations between these two blocks to reduce the off-diagonal coupling elements $\Gamma_{\sigma\sigma^*}$ to zero,

the density matrix is transformed to block-diagonal form. In SCF-MO theory these two blocks must correspond to *localized* molecular orbitals (LMOs),¹⁶ since the trace of the transformed $\Gamma_{\sigma\sigma}^{\text{LMO}}$ equals the number of electrons.

The resulting natural localized molecular orbitals (NLMOs)³⁴ have been shown to be in good agreement with LMOs calculated by the Edmiston-Ruedenberg^{16a} or Boys^{16b} methods, but with greatly improved computational efficiency. The NLMO procedure leads simultaneously to sets of filled and empty LMOs that respectively span the occupied and virtual subspaces. In addition, the NLMO procedure can be applied to correlated wave functions beyond the SCF approximation (although in this case the occupancy of each NLMO will generally be different from two or zero). NLMO expansions have been used to compare the transferability of NBOs and LMOs from one molecule to another, leading to the conclusion that NBOs are inherently *more* transferable than LMOs (often by factors of 2–4), and thus that NBOs are in better correspondence with the transferable bond units of elementary valence theory.³²

The expression for each NLMO in terms of its parent NBO (cf. eq 4) lets one see directly the delocalizing effect of $\sigma \rightarrow \sigma^*$ interactions, leading to energy lowerings of the form (3). In the present context, one may look at *intermolecular* delocalization tails of the NLMOs as a direct manifestation of the noncovalent contribution ($E_{\sigma\sigma^*}$; cf. eq 2 and 4) to van der Waals bonding. For example, in the equilibrium water dimer, one of the oxygen lone pair LMOs is approximately expressible as

$$(n_0)_{\text{LMO}} \approx (n_0)_{\text{NBO}} + \lambda(\sigma^*_{\text{OH}})_{\text{NBO}} \quad (16)$$

where σ^*_{OH} is the proximate antibond of the adjacent monomer associated with the intermolecular $n_0 \rightarrow \sigma^*_{\text{OH}}$ interaction, and λ is the coefficient of the weak intermolecular “delocalization tail” of the lone-pair LMO onto the adjacent monomer. NLMOs thus provide additional evidence of the intermolecular delocalization effects that accompany formation of a van der Waals complex.

F. Hyperconjugative Interactions in NBO Analysis

The preceding discussion emphasizes that hyperconjugative $\sigma \rightarrow \sigma^*$ interactions play a highly important role in NBO analysis. These interactions represent the weak departures from a strictly localized natural Lewis structure that constitute the primary “noncovalent” effects. The $\sigma \rightarrow \sigma^*$ interactions are manifested in a variety of forms in NBO analysis: (i) direct variational energy lowering (and corresponding geometry changes) associated with the deletion of specific σ^* basis orbitals (cf. eq 2), or specific $\hat{F}_{\sigma\sigma^*}$ matrix elements; (ii) changes in second-order energies (cf. eq 3) associated with the $\hat{F}_{\sigma\sigma^*}$ interaction; (iii) changes in the natural populations q_σ and q_{σ^*} of the hyperconjugating orbitals (cf. eq 5 and 14); (iv) changes in the overlap integral $\langle \tilde{\sigma} | \tilde{\sigma}^* \rangle$ of associated pre-NBOs $\tilde{\sigma}$ and $\tilde{\sigma}^*$ (cf. eq 13); and (v) changes in the delocalization tails of LMOs (cf. eq 4 and 16). Some of these changes (i.e., those pertaining to Fock matrix elements) are specific to the SCF approximation,

but the remainder apply to correlated wave functions of any form or accuracy. Together, these changes in NBO parameters allow a very complete picture of a specific $\sigma \rightarrow \sigma^*$ interaction, ranging from its quantitative numerical value or effect on the optimized molecular geometry to its qualitative origin in the shape or diffuseness of the associated orbitals.

The earliest applications of NBO analysis were to *intramolecular* noncovalent effects, particular those associated with the origins of barriers to internal rotation (cf. sections III.E and IV.B). Many of the regularities of $\sigma \rightarrow \sigma^*$ interactions were first established in the intramolecular context, where the relative separations and orientations of the σ and σ^* orbitals are constrained by the covalent linkages that form the molecule. A considerable variety of intramolecular stereoelectronic effects and bonding phenomena have subsequently been analyzed with NBO techniques (e.g., ref 35–41). The general success of NBO analysis in treating these phenomena provides additional evidence for the validity and conceptual utility of the method and for the pervasive role of $\sigma \rightarrow \sigma^*$ interactions in chemistry.

However, it was natural to conjecture that the unfilled valence-shell σ^* orbitals might also play an important role in *intermolecular* interactions. The intermolecular $\sigma \rightarrow \sigma^*$ interactions could be expected to be particularly important when the σ^* acceptor orbital presents a smooth, nodeless aspect (rather than, say, the highly noded “backside” of an sp^3 hybrid) toward a prospective donor σ orbital. Among covalently bonded molecules, this requirement is uniquely satisfied by σ^*_{AH} *hydride* antibonds, particularly when the electronegativity of A leads to strong polarization of σ^*_{AH} toward the outer (s-type, hydrogen) end of the orbital. The best *donor* orbital for such an interaction would be expected to be a diffuse lone pair n_D . From the shapes of these orbitals, simple maximum-overlap considerations would suggest that the $n_D - \sigma^*_{\text{AH}}$ interaction is optimized in linear “end-on” arrangements (as pictured, e.g., in Figure 4a). The prerequisite for a strong intermolecular hyperconjugative ($n_D \rightarrow \sigma^*_{\text{AH}}$) interaction could thus be expected to involve linear arrangements of the form D···H–A, the characteristic arrangement of hydrogen bonding. The systematic investigation of this simple conjecture is the subject of the present review.

III. Intermolecular Donor-Acceptor Models Based on NBO Analysis

A. H-Bonded Neutral Complexes

1. Water Dimer

The first natural bond orbital analysis on a hydrogen-bonded complex was carried out on the water dimer by Horn, Weinstock, and Weinhold⁴² at the semi-empirical INDO level of theory. The complexation energy ΔE was decomposed into $\Delta E_{\sigma\sigma}$ and $\Delta E_{\sigma\sigma^*}$ components. The $\Delta E_{\sigma\sigma}$ was found to be repulsive and $\Delta E_{\sigma\sigma^*}$ to be strongly attractive at the equilibrium dimer distance. Charge transfer from one of the oxygen lone pairs, n , of the electron donor to the proximate OH antibond, σ^* , of the electron acceptor was found to be

TABLE III. Basis Set Dependence of Binding Energy and of Natural Bond Orbital Charge-Transfer Analysis: Water Dimer $\text{H}_2\text{O} \cdots \text{HOH}$,^a SCF Level (All ΔE Values Given in kcal mol⁻¹)

basis set ^b	$E(\text{H}_2\text{O})^c$	$E(\text{dimer})$	ΔE	ΔE_{CT}	$\Delta E_{\text{A} \rightarrow \text{B}}^d$	$\Delta E_{\text{B} \rightarrow \text{A}}^d$	q_{A}^e
STO-3G	-74.96290	-149.93394	-5.10	-12.09	-11.86	-0.24	+0.0192 (+0.0201)
4-31G	-75.90739	-151.82708	-7.72	-10.14	-9.90	-0.24	+0.0152 (+0.0298)
6-31G*	-76.01054	-152.03011	-5.67	-9.54	-9.27	-0.30	+0.0137 (+0.0264)
6-31G**	-76.02317	-152.05530	-5.62	-9.65	-9.37	-0.29	+0.0140 (+0.0287)
6-31++G**	-76.03050	-152.06899	-5.01	-10.40	-9.27	-1.18	+0.0111 (-0.0032)
6-31++G**(2d)	-76.03455	-152.07597	-4.32	-10.32	-9.16	-1.20	+0.0110 (-0.0064)
TZP	-76.05589	-152.11932	-4.73	-6.58	-6.23	-0.38	+0.0086 (+0.0059)
TZP++	-76.05662	-152.12075	-4.71	-6.63	-6.27	-0.38	+0.0083 (+0.0032)
TZP++(2d)	-76.06005	-152.12662	-4.09	-6.51	-6.08	-0.47	+0.0081 (+0.0059)
HF limit	-76.068'		-3.9*				

^aAt fixed geometry. Intermolecular geometry from: Curtiss, L. A.; Pople, J. A. *J. Mol. Spectrosc.* 1975, 55, 1. Experimental water monomer geometry (0.957 Å, 104.5°). ^bSee ref 45 for precise specification of basis sets. Pure d-function sets were used in all cases except 6-31G* and 6-31G**, where Cartesian sets were used. ^cTotal SCF energies in au. ^d"A" refers to H_2O , and "B" refers to HOH, in $\text{H}_2\text{O} \cdots \text{HOH}$.

^eCharge on monomer " H_2O ", the proton acceptor, by natural population analysis. Values in parentheses are the corresponding Mulliken charges, shown for comparison purposes only. ^fPople, J. A.; Binkley, J. S. *Mol. Phys.* 1975, 29, 599. ^gPopkie, H.; Kistenmacher, H.; Clementi, E. *J. Chem. Phys.* 1973, 59, 1325.

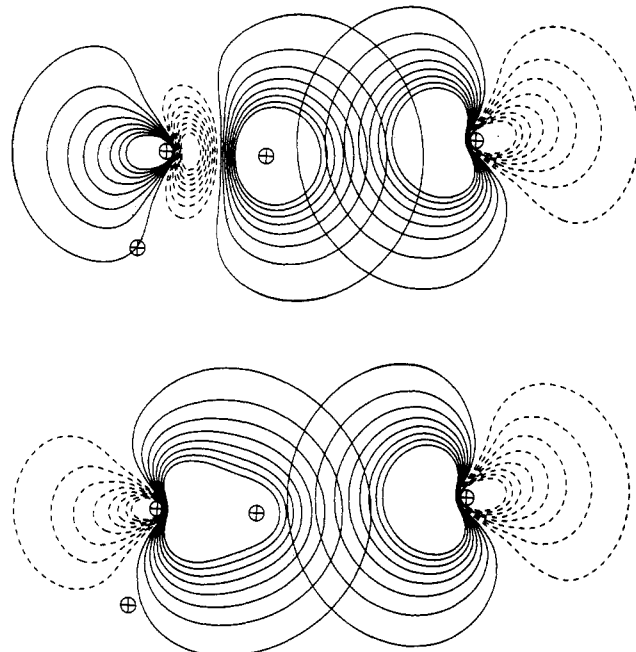


Figure 4. Contour plots of nonorthogonal pre-NBOs for the interacting oxygen lone pair n_{O} (right) with the OH antibond σ^*_{OH} (a, top) and bond σ_{OH} (b, bottom) of the equilibrium water dimer (RHF/6-31G* level), showing the significantly higher overlap associated with the attractive $n_{\text{O}} \rightarrow \sigma^*_{\text{OH}}$ interaction than with the repulsive $n_{\text{O}} \rightarrow \sigma_{\text{OH}}$ interaction. The positions of the atoms in the plane are given by the crosses, the two hydrogens of the electron donor water monomer (at the right) being out-of-plane. The outermost contour is at 0.002 au, corresponding roughly to the empirical van der Waals radius [Bader, R. W. F.; Henneker, W. H.; Cade, P. E. *J. Chem. Phys.* 1967, 46, 3341], and the contour interval is 0.03162 au (for clarity, only the outermost eight contour lines are shown).

of critical importance. This NBO study was extended to the ab initio SCF level by Weinstock and Weinhold^{43,44} with minimal and double- ζ basis sets. Though the quantitative details were somewhat altered, the essential picture of the water dimer hydrogen bond as an $n \rightarrow \sigma^*$ "charge-transfer" (CT) interaction was found to be valid.

Subsequently, higher levels of theory confirmed the $n \rightarrow \sigma^*$ picture.^{8,45} This was first done with a basis of better than double- ζ plus polarization quality and experimental H_2O monomer geometries.⁸ A more systematic study of the basis set dependence of the NBO

analysis of the water dimer was then carried out.⁴⁵ Both of these studies showed that the $n \rightarrow \sigma^*$ picture of the H-bond of the water dimer is stable with respect to basis set extension. The results for a series of basis sets are given in Table III. The largest calculation employed a triple- ζ plus polarization basis set with diffuse functions added to all atoms and a second set of d functions added to the oxygens, denoted as TZP++(2d). This basis yielded a monomer energy only 0.008 au from the Hartree-Fock limit for water and gave a water dimer complexation energy (-4.1 kcal/mol) only 0.2 kcal more negative than the estimated Hartree-Fock limit.

The complexation energy is decomposed as follows into charge-transfer (CT) and no-charge-transfer (NCT) parts:

$$\Delta E = E(\text{dimer}) - E(\text{isolated monomers}) = \Delta E_{\text{NCT}} + \Delta E_{\text{CT}} \quad (17)$$

Since charge-transfer interactions are associated with occupancy shifts from the manifold of filled orbitals of one monomer to the unfilled orbitals of the other, ΔE_{CT} can be estimated (in HF theory) by deleting Fock matrix elements connecting these manifolds and noting the change in the total energy. In effect, the charge-transfer component ΔE_{CT} is evaluated as the variational energy lowering due to expanding the variational space on each monomer to include unfilled orbitals on the other monomer. In addition, one can follow the details of CT through the natural population changes in individual NAOs and NBOs, or the net charge q transferred between monomers, for wave functions at and beyond the HF level. The remaining part of the binding energy, ΔE_{NCT} in eq 17, is due to exclusion repulsion and electrostatic (induction and polarization) interactions.

The largest basis set calculation on the water dimer, HF/TZP++(2d), gave values of -4.1, +2.4, and -6.5 kcal/mol for ΔE , ΔE_{NCT} , and ΔE_{CT} , respectively. The second-order perturbative analysis (eq 3) of the Fock matrix revealed only a single intermolecular stabilization interaction of greater than 0.25 kcal/mol in magnitude: the proximate $n \rightarrow \sigma^*$ interaction, with off-diagonal Fock matrix element 0.0864 au and energy denominator 1.42 au, yielding a second-order estimate of -6.6 kcal/mol, in rough agreement with the value (-6.5) of ΔE_{CT} . Accordingly, the NBO occupancies indicate that the proximate σ^* orbital has increased in occupancy by 0.0083 e from its monomer value of 0.0000

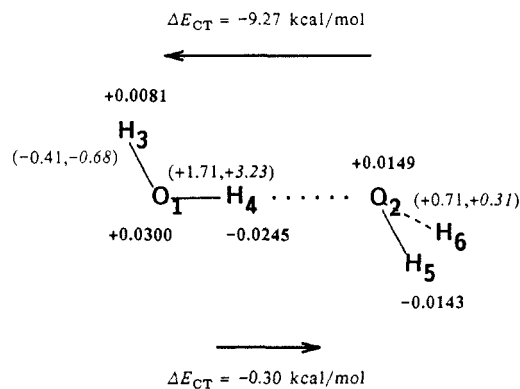


Figure 5. Summary of NBO charge-transfer analysis for equilibrium water dimer (RHF/6-31G* level), showing the net atomic charge (bold) on each atom, the energy change ΔE_{CT} associated with charge transfer in each direction, and (in parentheses) the NBO bond polarization and hybridization changes associated with formation of the complex. The first number in parentheses represents the percentage change in the bond polarization toward oxygen (e.g., the O₁-H₄ bond becomes 1.71% more strongly polarized toward O₁) and the second number (italics) represents the percentage change in s character of the oxygen bonding hybrid (e.g., the O₁ bond hybrid of the O₁-H₄ bond gains 3.23% in s character). For an isolated water monomer, the natural atomic charges are +0.478 on H and -0.957 on O, the OH bond is 73.96% polarized toward O, and the oxygen bonding hybrid has 23.76% s character. The changes in bond polarization and hybridization accompanying complex formation are associated with changes in monomer bond angles and lengths that are readily rationalized in terms of Bent's rule³³ and the distinct radii of s and p orbitals.

and that the proximate lone pair has decreased in occupancy by 0.0081 e from its monomer value of 1.9988. The total net value of transferred charge, by natural population analysis, was found to be 0.0081 e (from the first to the second monomer in H₂O...HOH; see Table III). Figure 4 shows contour diagrams (for the overlapping pre-NBOs, RHF/6-31G* level) of the hyperconjugative n_O-σ*_{OH} and the repulsive n_O-σ_{OH} orbital interactions of the water dimer at its equilibrium geometry.

Charge transfer not only results in an increase in binding energy but also allows a significant amount of exclusion repulsion to be overcome, allowing the molecules to approach each other more closely and to significantly penetrate the van der Waals contact distance (cf. Figure 4b). To test the magnitude of this effect, the H-bond distance in the water dimer was reoptimized at the HF/TZP level with CT deleted.⁴⁵ With the same geometry as in Table III, the H-bond length was found to stretch by 0.56 Å with deletion of the CT stabilization, the optimum value of ΔE_{NCT} being -2.44 kcal/mol. The ΔE_{NCT} is significantly less in magnitude than the full SCF value of ΔE in this basis set (-4.73 kcal/mol) and the O...H distance in the NCT structure, 2.60 Å, is equal to the sum of the Pauling van der Waals radii for O and H. Thus, in the absence of CT interactions, the remaining electrostatic interactions would not allow the monomers to approach each other very closely, and the binding energy would be significantly less. Electrostatic stabilization is nevertheless an important component of the binding energy, and it is enhanced as CT allows the monomers to approach each other more closely.

The changes of the atomic populations and the forms of the NBOs are given in Figure 5 for the water dimer. In order to become a better electron donor, the bonds

of the donor monomer become more polarized toward oxygen (0.7%), this being the origin of the population increase at O₂ and decrease at H₅ and H₆. There is an associated increase in the s character of the bonding hybrids on O₂ (0.3%), in accordance with Bent's rule.³³ This results in an increase in the percent p character of the oxygen lone pair, slightly increasing its diffuseness and overlap with the acceptor antibond and raising its energy. By far the largest changes occur in the H-bonded σ_{OH} NBO, σ(O₁H₄), which strongly increases in polarity and in oxygen hybrid s character. Increasing the polarization of this bond results in a corresponding increased polarization of the antibond toward H₄, making it a better acceptor (allowing increased overlap with the donor lone pair; cf. Figure 4a). Perhaps even more importantly, this bond polarization increase will result in a decrease of the repulsive lone pair-bond interaction of the H bond (Figure 4b). This change in the σ_{OH} NBO is clearly the origin of the decrease of electron density at and around the H end of the H bond,^{5b} charge transfer into the acceptor σ* NBO acting only partially to counteract this decrease. The decrease in polarization and percent s oxygen hybrid character of the other bond (O₁-H₃) of the acceptor monomer is simply a consequence of the sharp increases in these values in the H-bonded σ_{OH} NBO. Thus, there are significant intramolecular changes in electronic structure that are strongly coupled with the intermolecular charge-transfer interaction of the H bond. Similar results are found at higher levels of theory.⁴¹

The n → σ* CT picture of the water dimer was tested with a correlated wave function (i.e., beyond Hartree-Fock).⁴⁵ The correlation contribution to the water dimer binding energy is about 1 kcal/mol, or about 20% of the total binding energy, and mainly represents intermolecular dispersion energy. The method of configuration interaction with single and double substitutions at the 6-31G* basis set level (CISD/6-31G*) was used and indicated that the total amount of transferred charge increased somewhat and that the occupancy changes of individual NBOs upon complexation were consistent with the n → σ* picture, keeping in mind the significantly increased antibond and Rydberg occupancies resulting from correlation effects.

2. OC...HF and CO...HF

The structure and energetics of the isomeric H-bonded complexes OC...HF and CO...HF have been investigated by ab initio molecular orbital theory.⁴⁶⁻⁴⁸ Only with the inclusion of electron correlation is a significant preference for the experimentally⁴⁹ observed OC...HF isomer found. The large effect of correlation upon the relative stability of the two isomers is apparently entirely an electrostatic effect caused by the correlation-induced sign reversal of the dipole moment of CO.^{48,50} Two opposing views as to the origin of the H-bonding in the OC...HF and CO...HF complexes have been presented. Benzel and Dykstra^{46,47} and Spackman⁵⁰ have suggested that the interaction forces in these complexes are dominated by electrostatics. In our work using NBO analysis, we have found that "charge-transfer" effects are highly significant. In addition, a simple electrostatic model was found to be inadequate to account for the principal features of these complexes and their relative stability. In this section,

TABLE IV. NBO Analysis of CO:HF Complexes at the HF/6-31G* Level^a

	CO...HF	OC...HF
At Optimum HF/6-31G* Geometry		
R_{eq}	2.15 Å	2.26 Å
ΔE	-2.20	-2.92
ΔE_{CT}	-3.80	-10.02
$\Delta E_{NCT} = \Delta E - \Delta E_{CT}$	+1.60	+7.10
q	0.0034 e	0.0148 e
q , CISD/6-31G*	0.0045 e	0.0155 e
decomposition of ΔE_{CT}		
$\Delta E_{CT}(CO \rightarrow HF)$	-3.30	-9.20
$\Delta E_{CT}(HF \rightarrow CO)$	-0.52	-0.88
$\Delta E_{n\sigma^*}$	-3.14	-9.50
At Geometry Optimized with No Charge Transfer Present (NCT)		
R_{NCT}	2.80 Å	3.26 Å
$\Delta R_{CT} = R_{NCT} - R_{eq}$	0.65 Å	1.00 Å
ΔE (CT included)	-1.38	-1.13
ΔE_{NCT} (CT excluded)	-0.86	-0.61

^a All energy values are given in kcal/mol.

we summarize the results of the NBO analysis on OC...HF and CO...HF.

Table IV presents the NBO estimates of ΔE_{CT} and the net charge q transferred between monomers (determined by natural population analysis) for the two complexes at the HF/6-31G* level. As can be seen from the table, the total charge-transfer stabilization ΔE_{CT} is more than 6 kcal/mol greater in OC...HF than in CO...HF at the HF/6-31G* equilibrium geometry. This offers a clear explanation for how the severe repulsion⁵¹ in the optimum OC...HF structure is overcome to make this structure more energetically favorable than the optimum CO...HF structure. (While the 6-31G* results are subject to superposition error, similar conclusions are found for much larger basis sets.⁴⁸)

Insight into the nature of the charge transfer is obtained by the decomposition of ΔE_{CT} as presented in Table IV. The charge transfer is predominately in the direction from CO to HF. The largest single contribution to ΔE_{CT} can be identified with the matrix element $\langle n|\hat{F}|\sigma^*_{HF} \rangle$ between the proximate lone pair of the donor CO monomer (n_C or n_O for OC...HF or CO...HF, respectively) and the unfilled antibond σ^*_{HF} of the acceptor HF monomer. When this single element of the Fock matrix is set to zero and all other elements are left unchanged, the energy denoted by $\Delta E_{n\sigma^*}$ is obtained, which is -3.14 kcal/mol for CO...HF and -9.50 kcal/mol for OC...HF. The dominance of this $n \rightarrow \sigma^*$ interaction is consistent with the general picture of hydrogen bonding derived from the analysis of the water dimer.

Most of the preference for OC...HF can be traced to the competing donor properties of carbon and oxygen lone pairs. The $\Delta E_{n\sigma^*}$ term may be approximated by a second-order energy expression like eq 3 for each isomer

$$\Delta E_{n\sigma^*}(OC \cdots HF) = -2 \frac{\langle n_C|\hat{F}|\sigma^*_{HF} \rangle^2}{\epsilon_{\sigma^*_{HF}} - \epsilon_{n_C}} \quad (18)$$

$$\Delta E_{n\sigma^*}(CO \cdots HF) = -2 \frac{\langle n_O|\hat{F}|\sigma^*_{HF} \rangle^2}{\epsilon_{\sigma^*_{HF}} - \epsilon_{n_O}} \quad (19)$$

where ϵ_i is a diagonal NBO matrix element of the Fock operator \hat{F} . The estimates (18) and (19) give values of -10.6 and -2.8 kcal/mol, compared to the values -9.5 and -3.1 kcal/mol of Table IV. The rather large size

of these interactions leads to significant nonadditivity (of the order of 7–10%), reflecting the importance of third-order terms. The expressions show that the charge-transfer preference for OC...HF can be largely attributed to the better donor properties of n_C , as manifested in its higher energy ($\epsilon_{n_C} = -0.66$ au versus $\epsilon_{n_O} = -1.40$ au) and greater diffuseness, leading to stronger matrix elements with the acceptor antibond $\langle n_C|\hat{F}|\sigma^*_{HF} \rangle = 0.109$ vs $\langle n_O|\hat{F}|\sigma^*_{HF} \rangle = 0.069$ au), even though the C...H distance in OC...HF is 0.11 Å longer than the O...H distance in CO...HF.

The effects of charge transfer on the structure and energetics of the CO...HF and OC...HF complexes are also seen when the intermolecular distance of each isomer is optimized in the absence of charge transfer by deleting the corresponding intermolecular Fock matrix elements as described above. The no-charge-transfer (NCT) values so obtained are denoted R_{NCT} and listed in Table IV. As should be expected, the geometry change caused by charge transfer, $\Delta R_{CT} = R_{NCT} - R_{eq}$, is significantly greater for the carbon-bonded isomer than for the oxygen-bonded isomer: 1.00 versus 0.65 Å. These results demonstrate the importance of charge transfer in stabilizing neutral molecules that are within van der Waals contact. From Table IV, the binding energies with the charge-transfer effect deleted ($\Delta E_{NCT} = \Delta E - \Delta E_{CT}$) for the NCT structures are significantly smaller in magnitude (and favor the wrong isomer) as compared with the $\Delta E(R = R_{eq})$ values of the structures optimized with charge transfer allowed: -0.86 versus -2.20 kcal/mol for CO...HF, and -0.61 versus -2.92 kcal/mol for OC...HF.

As in the case of the water dimer, the major effect of the charge-transfer interaction is to allow the interacting molecules to move much closer to each other than would be possible if the interaction between the molecules were purely electrostatic in nature. This charge-transfer-enabled closer approach of the two molecules will in turn increase the electrostatic energy. It is, therefore, quite misleading to evaluate in some manner an electrostatic interaction energy between two molecules at an equilibrium geometry, and, finding that its magnitude is similar to the total binding energy, draw the conclusion that the interaction is mainly electrostatic in nature. We may speak of $\Delta E(R_{eq}) - \Delta E_{NCT}(R_{NCT})$ as the total net effect of charge transfer on the binding energy. Though much smaller in magnitude than $\Delta E_{CT}(R_{eq})$, this net effect of charge transfer is significant [at the HF/6-31G* level, $\Delta E(R_{eq}) - \Delta E_{NCT}(R_{NCT})$ is -1.34 and -2.31 kcal/mol for CO...HF and OC...HF, respectively] and seems to provide by far the most important contribution to the general features of the complex, especially the short equilibrium distances characteristic of hydrogen-bonded species.

The conclusions drawn from the HF/6-31G* level concerning the importance of charge transfer are essentially unchanged when the most accurate wave functions, i.e. larger basis sets and correlation energy,⁴⁸ are employed, just as in the case of the water dimer.

3. Complexes of NO and HF

An interesting comparison and contrast with the closed-shell CO:HF isomers is provided by the open-shell complexes of HF with the nitric oxide free radical.⁵² Investigation of NO:HF was stimulated by ob-

servations of Crim and co-workers on the gas-phase vibrational relaxation of HF.⁵³ Such studies indicate that NO is a remarkably efficient collision partner in relaxing HF (e.g., about an order of magnitude more efficient than CO), suggesting the formation of long-lived collision complexes of NO and HF in which HF vibrational excitation is efficiently quenched. Since NO and CO have rather similar dipole moments (0.153 vs 0.112 D), rotational constants (1.70 vs 1.93 cm⁻¹), and molecular weights, there are apparently important *chemical* differences in their collision complexes with HF.

The donor-acceptor picture readily suggests some qualitative features of the NO:HF potential energy surface. NO differs from CO by addition of an electron to a π^* orbital, resulting in the NBO configuration

$$(\sigma_{NO})^2 (\pi_{NO})^3 (n_O)^2 (n_N)^2 (n_O^\perp)^1 (n_N^\perp)^1$$

where n_O^\perp and n_N^\perp denote the p-type components of the former π bond, and n_O and n_N denote the σ -type lone pairs along the internuclear axis. As the analogy to CO would indicate, HF can form distinct linear isomers by H-bonding to either the nitrogen end ($n_N \rightarrow \sigma^*_{HF}$) or oxygen end ($n_O \rightarrow \sigma^*_{HF}$) of the NO. Since N is more electronegative than C, the linear ON...HF isomer is somewhat weaker than the analogous OC...HF complex.

However, the additional electron in the π^*_{NO} system implies that NO also has significant donor capacity for nonlinear H bonds to HF ($n_N^\perp \rightarrow \sigma^*_{HF}$, $n_O^\perp \rightarrow \sigma^*_{HF}$ bonding). Thus, compared to CO, NO has the additional capacity to form "half-H-bonds" with HF over a wide range of approach angles, and so offers a considerably larger "acceptance angle" for binding to HF. Since the n_N^\perp and n_O^\perp orbitals are essentially p type, these orbitals have considerable donor strength compared to the s-rich n_N and n_O σ -type lone pairs.

This picture can be sharpened in terms of the "different hybrids for different spins" open-shell NBO description.¹³ The α (majority) and β (minority) natural Lewis structures are as follows:



The β -spin set favors the two linear structures (analogous to the isovalent :C=O: molecule), whereas the carbonyl-like α -spin system evidently favors bent ($\sim 120^\circ$) structures of the form



In fact, for *any* approach angle $\chi = \angle_{HNO}$ or \angle_{HON} in the interval $0^\circ < \chi < 180^\circ$, the α -spin Lewis structure can rehybridize (at little energetic cost) to point a donor n_N^\perp or n_O^\perp orbital toward the hydride σ^*_{HF} acceptor orbital. In agreement with this qualitative picture, the FH...NO potential surface is found to exhibit net binding for FH approaching at *any* angle around the NO (unlike the case of CO:HF, where attractive wells are concentrated around the linear approach directions). Thus, the added electron of NO "unlocks the Lewis structure" to allow more flexible deployment of n donor orbitals for strong n $\rightarrow \sigma^*_{HF}$ interactions with HF. The dramatic change in the "acceptance angle" for H-bonding accounts simply for the increased efficiency of NO in

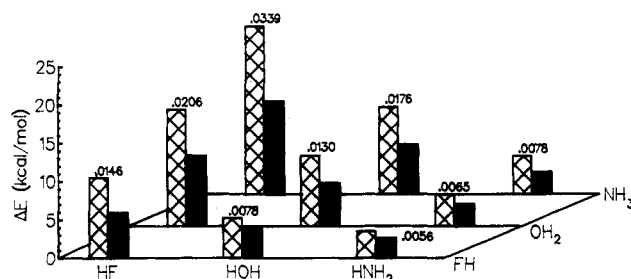


Figure 6. Graphical summary of NBO analysis for H-bonded complexes involving NH₃, H₂O, and HF, showing the trends in charge-transfer energy ΔE_{CT} (hatched bar), total binding energy ΔE (solid bar), and net charge q transferred between the species (printed number). For each A-H...B complex, the Lewis acid (acceptor) A-H is along the forward axis and the Lewis base (donor) B is along the receding axis. Note that ΔE_{CT} significantly exceeds the net ΔE in all the H-bonded complexes and that ΔE_{CT} , ΔE , and q vary smoothly with Lewis acid-base strength (electronegativity differences) of the monomers in the expected way. (Data from Table VI, ref 45.)

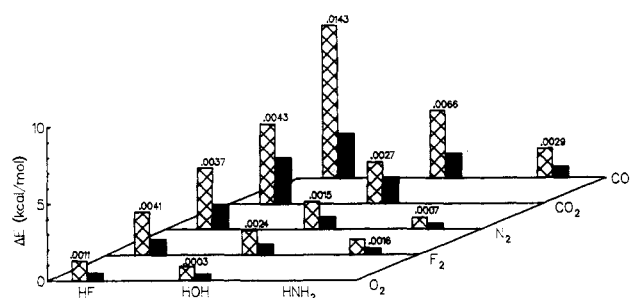


Figure 7. Similar to Figure 6, for H-bonded complexes between Lewis acids HF, HOH, or HNH₂ and Lewis bases CO, CO₂, N₂, F₂, or O₂. (Data from Table IV, ref 45.)

forming long-lived collision complexes with HF. Further details of the NBOs and the potential surface are presented in ref 52.

The striking difference in angular properties of CO:HF and NO:HF complexes is further evidence for the important role of *chemical* forces in van der Waals bonding. While such differences would seem difficult to rationalize on electrostatic grounds, they have a simple, intuitive explanation in the donor-acceptor picture.

4. Survey of a Large Series of H-Bond Complexes

The general importance of n $\rightarrow \sigma^*$ and other forms of CT stabilization in intermolecular interactions has been examined by NBO analyses on a large series of H-bonded complexes at the HF/6-31G* level, using optimized intermolecular geometries. All dimer combinations A...B between A = N₂, O₂, F₂, CO₂, CO, HF, H₂O, and NH₃ and B = HF, H₂O, and NH₃ were investigated. This study was reported in detail in ref 45. In this section, we report a summary of the results. In section III.B, the results from the study for the non-hydrogen-bonded complexes in this series are summarized. Figure 6 illustrates the results of the charge-transfer analysis for the hydrogen-bonded complexes between the hydrides. Figure 7 illustrates the results for hydrogen-bonded complexes between the hydrides and the diatomics OC, O₂, N₂, and F₂ and the triatomic CO₂. In all of the H-bonded complexes, ΔE_{CT} is sig-

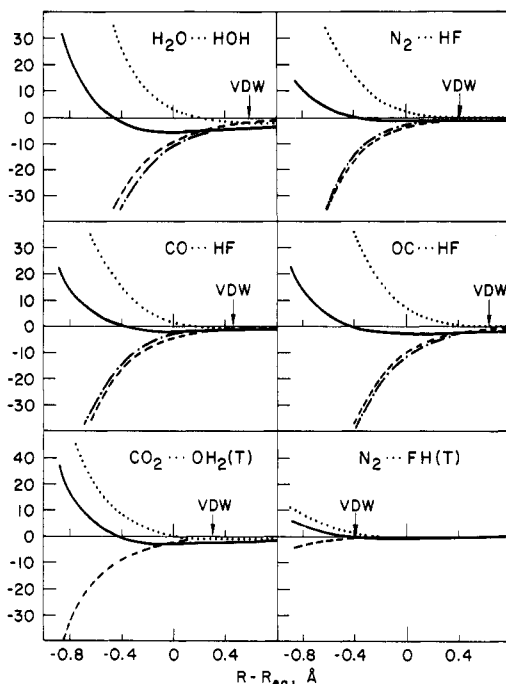


Figure 8. RHF/6-31G* values of ΔE (—), ΔE_{CT} (---), $\Delta E_{n\sigma}^{(2)}$ (—·—), and ΔE_{NCT} (···) plotted as a function of displacements from the equilibrium intermolecular separation, $R - R_{eq}$, for some H-bonded (upper four) and non-H-bonded (lower two) complexes. The energies are denoted in kcal/mol on the ordinates. The arrow denotes the distance of van der Waals contact. (Reproduced from ref 45; copyright 1986 American Institute of Physics.)

nificantly greater in magnitude than ΔE . That ΔE_{CT} is greater than ΔE in the hydrogen-bonded interactions is consistent with the results for the water dimer and the CO:HF complex.

It is important in this context that the charge-transfer and exclusion repulsion energies both vary exponentially with distance. Hence, as the CT interactions increase, more repulsion can be overcome and more penetration of the van der Waals distance, d_p , is possible. In the complexes of each donor monomer (A), the magnitudes of both the dominating $\Delta E_{A \rightarrow B}$ and the much smaller $\Delta E_{B \rightarrow A}$ increase strongly, as does d_p , when the acceptor monomer is progressively changed from HNH_2 to H_2O to HF. Contributions to ΔE_{CT} from individual orbital interactions can be estimated from the NBO Fock matrix by the second-order perturbation theory described previously. These second-order estimates show that the dominant contribution to ΔE_{CT} and to $\Delta E_{A \rightarrow B}$ arises, in each H-bonded complex, from a single $n \rightarrow \sigma^*$ interaction. This single contribution, $\Delta E_{n\sigma}^{(2)}$, was found (except in a few of the weaker cases) to be 1 or 2 orders of magnitude greater than any other second-order contribution in the hydrogen-bonded complexes.

Unless there is significant CT in both directions, the total charge transferred q is a useful measure of the importance of CT. The relative magnitudes of $\Delta E_{A \rightarrow B}$ and $\Delta E_{B \rightarrow A}$ indicate whether the CT is predominantly in one direction. One of the most important findings derived through the NBO method is that seemingly small values of transferred charge (0.001–0.01 e) are associated with energy stabilizations of chemical significance. A proportionality of roughly unity between the quantity of charge transferred into an orbital and the energy stabilization (in atomic units) associated with

the transfer has been found (cf. eq 5). A charge transfer of merely 0.01 e will thus have an associated ΔE_{CT} of around 6 kcal/mol. Except where the CT is not overwhelmingly in one direction, this rough “rule of thumb” holds up very well. The NBO method gives values for q that are usually significantly smaller (and never larger) in magnitude than the Mulliken values at the HF/6-31G* level. The Mulliken values for q have a much greater basis set sensitivity.

Figure 8 illustrates the variations of ΔE , ΔE_{CT} , and ΔE_{NCT} as a function of internuclear separation R for four H-bonded complexes ($H_2O \cdots HOH$, $CO \cdots HF$, $OC \cdots HF$, $N_2 \cdots HF$) at the HF/6-31G* level with 6-31G*-optimized monomer geometries. The “no-charge-transfer” term ΔE_{NCT} represents the effects (steric repulsion, electrostatic, internal polarization, etc.) of terms other than charge transfer. There is a single dominant interaction of $n \rightarrow \sigma^*$ type in each H-bonded complex in Figures 6 and 7. Hence, for the four H-bonded complexes considered here we have shown in Figure 8 the values of $\Delta E_{n\sigma}^{(2)}$, the second-order estimate of the $n \rightarrow \sigma^*$ interaction energy. Marked on the axis of each plot in Figure 8 is the value of the empirical van der Waals contact distance R_{vdW} . At this distance, repulsions of the closed-shell monomers would be expected to become significant.

As Figure 8 shows, the variations of the NBO charge-transfer term with internuclear distance are smooth, exhibiting no anomalies or artifacts at the equilibrium distances and having the general behavior expected on physical grounds. The term ΔE_{NCT} generally exhibits weak attractions at larger R (presumably of electrostatic origin) but starts rising near R_{vdW} in the approximately exponential manner associated with steric forces. For the H-bonded species, the CT term ΔE_{CT} (dominated by $\Delta E_{n\sigma}^{(2)}$) is negligible in the long-range region but leads to a strong attractive contribution that pulls the monomers into the observed equilibrium distances. It can be seen that the simple second-order estimate $\Delta E_{n\sigma}^{(2)}$ closely tracks the total ΔE_{CT} in each H-bonded complex. The NBO analysis is thus found to give a consistent picture of the bonding in this entire series of complexes in terms of CT interactions, showing a close correlation of these interactions with the van der Waals penetration distance and the dissociation energy of the complex.

The orderings of Lewis base (electron donor) and Lewis acid (electron acceptor) strength among these molecules are in accord with chemical intuition and are qualitatively understandable on the basis of orbital overlap and energy considerations.

5. Cooperativity in H-Bonding

Cooperativity effects in clusters seem to be generally associated with donor-acceptor interactions where a monomer can participate concertededly as a donor and acceptor. Neutral water clusters are a good example of this. The NBO analysis of the charge distributions in the water dimer (see Figure 5 and related discussion in section III.A.1) shows why it is easy to predict that in a H-bonded network, such as ice, where each molecule acts twice as an electron donor and twice as an electron acceptor, all of the OH bonds will significantly increase in polarity and oxygen hybrid s character. Such changes enhance both the acceptor and donor

TABLE V. Natural Atomic Charges and Forms of σ NBOs in Cyclic Water Polymers (H_2O) $_n$ ($n = 3-6$), with the Corresponding Values for $n = 1$ (Monomer) and $n = 2$ (Electron Acceptor Monomer or Dimer) Also Given^a

	$n = 1$	$n = 2$	$n = 3$	$n = 4$	$n = 5$	$n = 6$
ΔE		-5.73	-15.58	-36.13	-50.96	-61.90
$\Delta E/n$		(-5.73)	-5.19	-9.03	-10.19	-10.32
			Binding Energies			
O	-0.381	-0.433	-0.441	-0.461	-0.469	-0.470
H'	+0.191	+0.220	+0.258	+0.279	+0.288	+0.290
H''	+0.191	+0.168	+0.183	+0.182	+0.181	+0.179
			NBOs			
$\sigma(\text{O}-\text{H}'')$						
% pol	59.54	62.41	64.98	67.70	68.64	68.76
% s	14.33	16.28	17.20	18.78	18.93	18.63
$\sigma(\text{O}-\text{H}')$						
% pol	59.54	58.42	59.17	59.09	59.03	58.95
% s	14.33	14.24	14.01	13.72	13.55	13.53

^a In the cyclic polymers, all water molecules are equivalent. The H-bonded hydrogens are denoted as H' and the non-H-bonded hydrogens as H''. For the σ NBOs, the percent polarization toward oxygen and the percent s character of the oxygen hybrid are given. Basis set is STO-4G; structures from ref 54. Binding energies are in kcal/mol and differ slightly from those in ref 54 due to the use of water-optimized STO-4G scale factors in that work.

abilities of the molecule. The enhanced negative charge at O₁ in the water dimer and the significantly decreased s character (and hence, increased p character) of the σ -type lone pair on O₁ mean that the electron-donor ability of the H₄-O₁-H₃ monomer will be significantly enhanced over that of an isolated monomer. Clearly, these changes in monomer orbitals also result in enhancement of dipole-dipole electrostatic interactions between the water molecules and also allow the H-bond distance to further decrease. Thus, CT interactions will strongly contribute to the observed cooperativity in H-bonding that occurs upon forming chains or networks of H bonds. We illustrate the strong changes that can occur in monomer σ bonds and atomic charges in Table V with data from NBO analyses of cyclic water polymers (up to the hexamer), using the optimized structures of Del Bene and Pople⁵⁴ and the minimal STO-4G basis set. The trends in this table are consistent with the effects discussed above. Finally, it is interesting that when one forms a one-dimensional (noncyclic) chain of H bonds, the middle monomers are nearly uncharged, and there is a strong transfer of charge from one end of the chain to the other. For instance, Kollman and Allen⁵⁵ find a charge transfer (Mulliken analysis, minimal basis level) of 0.054 e from one end to the other of a linear duodecamer of water. It is noteworthy that cooperative effects cannot be described by purely electrostatic models, since the Coulomb interaction involves only pairwise additive terms.

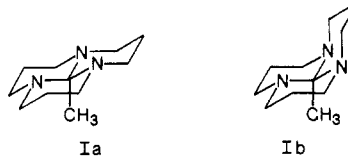
6. Hydrophobic Interactions

The nature of the interaction between hydrocarbons and water (the "hydrophobic effect") remains paradoxical after more than a century of intensive investigation.⁵⁶ The interactions of water with nonpolar groups of proteins are thought to be an important aspect of virtually all biophysical phenomena.⁵⁷ In the context of this review, the hydrophobic effect is of particular interest because nonpolar species inherently lack the leading multipole moments that would be considered necessary, in an electrostatic picture, for effective H-bonding. As Hvidt has noted,⁵⁸ "aqueous solutions of nonpolar molecules are notorious because

of their eccentric thermodynamic properties, and because of our limited understanding of the molecular interactions in the solutions".

The CH₄...OH₂ complex serves as the prototype for hydrophobic C-H...O bonding. Ungemach and Schaefer⁵⁹ examined this species at DZ and DZP levels of SCF theory and found that the interaction energy varies strongly with the choice of basis set. Their estimate of the H-bond energy ($\Delta E_{\text{HB}} \approx -0.5$ kcal/mol, including an estimated 0.1 kcal/mol correction for the neglected dispersion contribution) suggests that the hydrophobic C-H...O bond is very weak. Similar estimates of C-H...O strength have been adopted by others.⁶⁰

The question of the strength of C-H...O bonding was recently taken up again by Seiler et al.⁶¹ in the context of some remarkable features of the crystal structure of the tricyclic orthoamide **Ia**. Most surprising is the



observation that the methyl group is nearly *eclipsed* (N-C-C-H torsion angle of 8.0 (9°) in the hydrated form of the crystal, an apparently unprecedented result for an ethane-like C(sp³)-CH₃ conformation. In the crystalline hydrate, each orthoamide molecule is complexed via nitrogen atoms to a chair-like arrangement of six water molecules. Inspection of the crystal structure reveals that each C-H bond of the methyl group points nearly at an oxygen atom of a neighboring triad (C-H...O angle, 170°; H...O distance, 2.67 Å) in an arrangement suggestive of hydrogen bonding. Ab initio calculations of the torsional potential indicate that the isolated orthoamide molecule must substantially favor the usual staggered conformation (by ~5.5 kcal/mol). Experimentally, the methyl group is indeed found to revert to the normal staggered conformation in the anhydrous form of the crystal, whose unit cell consists of asymmetrically paired **Ia**, **Ib** orthoamide molecules. The clear indication of both theoretical and experimental results is that methyl-water H-bonding inter-

actions of quite surprising strength ($\sim 1.5\text{--}2$ kcal/mol per C-H...O unit) are acting to twist the methyl group out of its accustomed staggered conformation in the hydrated orthoamide. The possible biophysical implications of such hydration-specific control of an alkyl conformational preference are quite apparent.

Ab initio calculations and NBO analysis have been employed to investigate C-H...O H-bonding in the $\text{CH}_4\cdots\text{OH}_2$ complex and other model complexes [$\text{CH}_4\cdots\text{O}(\text{H})\text{H}\cdots\text{NH}_3$, $\text{H}_2\text{NCH}_2\text{CH}_3\cdots\text{O}(\text{H})\text{H}\cdots\text{NH}_3$, etc.] related to the hydrated orthoamide system, using highly extended basis sets and extensive treatment of correlation effects.⁶¹ Several noteworthy conclusions emerge from these studies:

(i) Correlation "corrections" to C-H...O bonding are truly dramatic. For example, the MP2/6-31G* C-H...O bond strength of ~ 1.6 kcal/mol corresponds to an approximate 160% correlation "correction."⁶² At all basis set levels the electron correlation effect is nearly an order of magnitude greater than the value (~ 0.1 kcal/mol) that had previously been estimated⁵⁹ on the basis of dispersion forces in systems of similar size (e.g., Ne...Ne).

(ii) Cooperative enhancement (section III.A.5) is found to be highly significant, amounting to at least 0.5–1.0 kcal/mol in the arrangements characteristic of the hydrated orthoamide. Thus, the nonadditive cooperative "corrections" may actually rival or surpass the binding energy of the $\text{CH}_4\cdots\text{OH}_2$ binary complex.

(iii) The optimized $\text{CH}_4\cdots\text{OH}_2$ geometry reveals many surprises. Contrary to the universal experience with other A-H...B hydrogen bonds,⁶³ the C-H bond of the C-H...O interaction is *shortened* and vibrationally *blue-shifted* with respect to the other C-H bonds of the complex (or of isolated CH_4). Although the H...O separation of the monomers is unusually large (providing somewhat improved mathematical justification for expansions of multipole type), the optimized structure exhibits its indifference to the leading terms of an electric multipole expansion by turning the water dipole nearly perpendicular to the C-H...O bond direction!

It might be supposed that such radically different properties of C-H...O hydrogen bonding would require a completely revised NBO picture of the origin of H-bonding, but this is not the case. The $n_0 \rightarrow \sigma^*_{\text{CH}}$ interaction (with $\Delta E_{n_0\sigma^*}^{(2)} \simeq 2$ kcal/mol) appears in typical fashion as the dominant contribution to bonding. Natural population analysis indicates net transfer of charge into the σ^*_{CH} antibond, as usual. It appears that the principal role of correlation effects is to reduce the steric repulsion of filled n_0 and σ_{CH} orbitals (e.g., by contracting the electron density to reduce the effective van der Waals radius of the C-H bond; cf. Figure 4b), thus allowing the ~ 2 kcal/mol hyperconjugative $n_0\cdots\sigma^*_{\text{OH}}$ interaction to fully assert itself.

The extreme sensitivity of C-H...O bonding to cooperativity effects may play an important role in the anomalous thermodynamic behavior associated with hydrophobic interactions. It is interesting that the most distinctive features of hydrophobic bonds may be associated with non-pairwise-additive cooperativity (and anticooperativity) effects that are inherently outside an electrostatic picture. Further studies of cooperatively enhanced hydrogen bonding in systems of biophysical interest are likely to be a fruitful area of application of the NBO donor-acceptor picture.

7. Other Topics

Brief mention should be made of the IR spectral features of H-bonded complexes, in relation to the donor-acceptor model. The formation of B...H-A hydrogen bonds is accompanied by significant IR spectral changes in the A-H stretching absorbance, which decreases in frequency (ν_{AH}) and increases (by an order of magnitude or more) in intensity.^{63,64} The decrease in ν_{AH} is consistent with the bond weakening associated with increased occupancy of the σ^*_{AH} orbital. The dramatic intensity enhancement is almost entirely due to the increase of the derivative of the molecular dipole moment with respect to displacement of the H-bond proton H_4 along the H-bond axis, $\partial\mu/\partial y(\text{H}_4)$, and the importance of charge transfer is indicated by the finding that the enhancement of $\partial\mu/\partial y(\text{H}_4)$ cannot be explained on the basis of an electrostatic model alone.⁶⁴ Zilles and Person^{64a} carried out a charge-charge flux-overlap analysis of the intensity enhancement and found that the dominant charge flux contribution to $\partial\mu/\partial y(\text{H}_4)$ was composed of nearly equal contributions from intramolecular polarization and intermolecular charge-transfer terms. Their division between intra- and intermolecular contributions was carried out in the framework of Mulliken population analysis, which is qualitatively similar (in the symmetric treatment of intermolecular overlap; see section IV) to NBO analysis, and thus would be expected to lead to a qualitatively similar decomposition of $\partial\mu/\partial y(\text{H}_4)$. The alternative analysis by Swanton, Bacska, and Hush^{64b} was based on an unsymmetric Morokuma-type treatment of the valence AO space (section IV) and again led to strong contributions from both electrostatic and charge-transfer interactions. Thus, charge transfer is found to be a prime factor in the intensity enhancement of ν_{AH} however one partitions valence AO space. Since many theoreticians strongly favor electrostatic over charge-transfer models of H-bonding, the above results were interpreted to mean that charge transfer is important *dynamically* (i.e., through its variation with vibration) but not *statically*.^{64b,65} Of course, no such paradoxical distinction is necessary in the donor-acceptor picture, since vibrational enhancement appears as a direct corollary of the essential charge-transfer nature of the H-bonding interaction.

Other experimental studies⁶⁶ involving IR spectral changes and other techniques have given important evidence concerning the role of covalency and cooperativity effects in H-bonding (cf. also sections III.A.6 and III.C.2). Huyskens^{66a} studied the factors governing the influence of a first hydrogen bond (with formation constant K_1) on the formation constant K_2 of a second hydrogen bond. For instance, H-bonding between two phenol molecules is significantly enhanced when the first phenol molecule is H-bonded (in $\text{PhOH}\cdots\text{NR}_3$ fashion) to an amine. If K_2° denotes the formation constant of the second H bond in the *absence* of the first H bond, then it is found that $\log(K_2/K_2^\circ)$ correlates much more favorably with $(-\Delta\nu_{\text{AH}})_1$, the A-H frequency shift due to the first H bond, than with the stability constant K_1 for formation of the first bond. Since this correlation is observed to persist *irrespective of the charge of the partners*, Huyskens concludes that "the influence of the first bond on the reactivity of the other sites has thus rather a covalent than an electro-

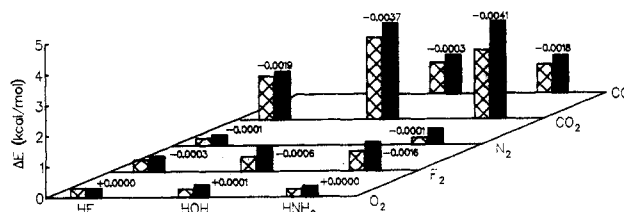


Figure 9. Similar to Figure 7, for non-H-bonded complexes between HF, H₂O, or NH₃ and CO, CO₂, N₂, F₂, or O₂. Note the many elements of dissimilarity (relative strength of ΔE and ΔE_{CT} , dependence on electronegativity differences, sign of q , etc.) that distinguish these complexes from the corresponding H-bonded complexes of Figure 7. (Data from Table V, ref 45.)

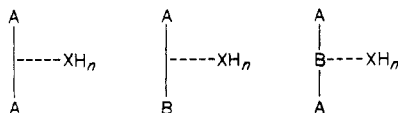
static character.^{66a} Additional experimental studies pertaining to H-bond cooperativity are described in ref 66b.

B. Non-H-Bonded Neutral Complexes

1. Survey of a Large Series of Non-H-Bonded Complexes

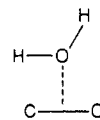
The importance of charge-transfer stabilizations in neutral molecular complexes not involving hydrogen-bond formation has also been examined by NBO analysis.⁴⁵ All dimer combinations A...B between A = N₂, O₂, F₂, CO₂, and CO and B = HF, H₂O, and NH₃ were investigated. The work was done at the HF/6-31G* level in a manner similar to the H-bonded complexes discussed in section III.A.4. Figure 9 compares ΔE and ΔE_{CT} for complexes that were found to have non-H-bonded structures in this series. The strong contrast with H-bonded complexes (Figures 6 and 7) is immediately evident.

Charge transfer is generally much less important in the non-H-bonded complexes than in the H-bonded complexes. This is indicated by the fact that ΔE is generally greater in magnitude than ΔE_{CT} . Although CT effects are smaller, there are some important trends to point out in the NBO CT analyses of these complexes. In the T-shaped complexes

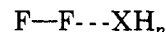


the only significant CT interaction would be of $n \rightarrow \pi^*$ type. The $n \rightarrow \pi^*$ interaction would, however, be zero when the acceptor monomer is a homonuclear diatomic since the $n \rightarrow \pi^*$ overlap would be zero. Diatomics (as CO) or triatomics (as CO₂) that have polarized π -systems should, however, act as significant π^* acceptors. These expectations are borne out by Figure 9, where one can see that, in the N₂, F₂, and O₂ T-complexes, q is of negligible magnitude (0.0001), whereas in the CO₂ T-complexes and the OC...NH₃ T-complex, q is of significant magnitude (0.0018–0.0042). In the former set of complexes, there are very weak nonspecific CT interactions in both directions that result in a net q of nearly zero. The latter set of T-complexes involving CO and CO₂, however, has a clear CT direction, with $\Delta E_{B \rightarrow A}$

significantly greater than $\Delta E_{A \rightarrow B}$. These could be called $n \rightarrow \pi^*$ complexes. The CO...OH₂ complex



although in some ways analogous to the other CO₂ and CO T-complexes, is unique in that it has nonnegligible CT of comparable magnitude in both directions. In this complex, H₂O is positioned such that it can act not only as a donor in an $n \rightarrow \pi^*$ interaction but also as a weak σ^* acceptor. Finally, the linear F₂ complexes with NH₃, H₂O, and HF



provide examples of weak, non-H-bond, $n \rightarrow \sigma^*$ CT interactions that grow progressively stronger as the donor into σ^* changes from FH to OH₂ to NH₃.

It may be noted that Morokuma-type analysis (section IV.B) had led to the conclusion that there is no clear distinction to be drawn between complexes of H-bonded and non-H-bonded type (the Morokuma "electrostatic" term being predictably dominant in all cases). In contrast, NBO analysis reveals a striking distinction between H-bonded (Figures 6 and 7) and non-H-bonded species (Figure 9), in accord with chemical evidence.

The variations of ΔE , ΔE_{CT} , and ΔE_{NCT} as a function of internuclear separation for two of the non-hydrogen-bonded complexes, the T-shaped CO₂...OH₂ and N₂...FH complexes, are shown in Figure 8. As in the case of the hydrogen-bonded complexes, the variations in ΔE_{CT} are smooth with no anomalies or artifacts at the equilibrium distance.

Peterson and Klemperer suggested⁶⁷ that the approximately 1 kcal/mol internal rotation barrier in CO₂...OH₂ might arise from the formation of a π -type bond through the interaction of the lone pairs of H₂O with the two π^* orbitals of CO₂. NBO analysis⁴⁵ showed, however, that this interaction is only about 0.2 kcal/mol (compared to the total barrier of 0.95 kcal/mol at the MP2/6-31G* level), due to the weak $\pi-\pi$ overlap at the intermolecular distance of ~2.8 Å. (In contrast, the much stronger σ -type CT interaction is about 3 kcal/mol, but of course gives no contribution to the rotation barrier.) Simple electrostatic models based on quadrupole-quadrupole interactions support the conclusion that the internal rotation barrier in CO₂...OH₂ is essentially electrostatic in nature.⁴⁵

2. Competition between H-Bonded and Non-H-Bonded Structures

We turn now to the question of the competition between H-bonded and non-H-bonded structures for this series of complexes. For this discussion we use the MP2/6-31G* energies from ref 45. By far the weakest of the complexes are those of O₂, which have a maximum binding energy of 0.8 kcal/mol. All of the other complexes have at least one structure with a binding energy of more than 1 kcal/mol.

There are some clear trends regarding the competition between H-bonded and non-H-bonded structures for the complexes of N₂, F₂, CO, and CO₂ with HF, H₂O,

TABLE VI. Natural Bond Orbital Charge-Transfer Analysis of Ion-Molecule Complexes (All ΔE Values Given in kcal mol⁻¹)

complex ^a	basis set	ΔE	ΔE_{CT}	$\Delta E_{\text{ion} \rightarrow \text{H}_2\text{O}}$	$\Delta E_{\text{H}_2\text{O} \rightarrow \text{ion}}$	$q_{\text{H}_2\text{O}}$
F ⁻ :H ₂ O	HF/6-31+G*	-23.1	-34.5	-34.1	-0.3	-0.048 (-0.037)
Cl ⁻ :H ₂ O	HF/6-31+G*	-11.6	-11.2	-11.0	-0.2	-0.023 (-0.031)
O ₂ ⁻ :H ₂ O	HF/6-31+G*	-17.3	-13.5	-13.5	-0.6	-0.029 (-0.021)
Li ⁺ :OH ₂	HF/6-31G*	-39.6	-7.2	-1.0	-6.7	+0.012 (+0.102)
Na ⁺ :OH ₂	HF/6-31G*	-28.6	-3.9	-0.7	-3.3	+0.008 (+0.074)
Mg ²⁺ :OH ₂	HF/6-31G*	-84.2	-14.1	-1.4	-13.1	+0.030 (+0.185)
Fe ⁴⁺ :OH ₂	b	-88.0	-27.5	-5.1	-22.9	+0.050 (+0.088)
Fe ³⁺ :OH ₂	b	-166.4	-70.1	-6.8	-62.3	+0.200 (+0.286)

^a Geometries: F⁻:H₂O and Cl⁻:H₂O are from: Kistenmacher, H.; Popkie, H.; Clementi, E. *J. Chem. Phys.* 1973, 58, 5627 (C₁X...HOH structures); O₂⁻:H₂O is from ref 75 (HF/6-31G* $^2\text{A}_2$ C_{2v} structure) Li⁺:OH₂, Na⁺:OH₂, and Mg²⁺:OH₂ are from HF/6-31G* optimizations of C_{2v} planar structures; Fe⁴⁺:OH₂ and Fe³⁺:OH₂ are C_{2v} planar structures described in ref 76b. ^b Basis set I in ref 76b.

and NH₃. The competition between isomeric structures for the complexes is strongly influenced by CT, which can be understood by very simple considerations of Lewis acid and Lewis base strength and the shapes of the participating orbitals. Electrostatic interactions play a subsidiary, though sometimes important, role. In all cases, the complexes with HF are H-bonded, these being favored over non-H-bonded structures by 0.9–2.2 kcal/mol. This trend is clearly due to the role of HF as a strong σ^* acceptor. Continuing this trend, N₂ and CO prefer H-bonded complexes with H₂O, but by smaller margins than that with HF. The linear non-H-bonded structure is slightly favored over the H-bonded one for F₂ with H₂O, evidently by a subtle balance of electrostatic, charge-transfer, and correlation effects. The case of CO₂ with H₂O is more clear-cut, with the non-H-bonded structure being favored by 1.3 kcal/mol over the H-bonded one. Note from Figures 7 and 9 that ΔE_{CT} is nearly identical for the two structures at -2.7 kcal/mol, revealing the comparable electron donor and acceptor strength of H₂O. This points to the presence of significantly more favorable electrostatic interaction in the T-shaped non-H-bonded structure, which is understandable on the basis of interactions of dipole and quadrupole moments. The σ^* acceptor strength of NH₃, however, is weak enough that H-bonded structures are not dominant in any of its complexes.⁶⁸ The H-bonded and non-H-bonded complexes of N₂ and CO with NH₃ are too close in binding energy to judge which are more stable. Continuing the trends started in the complexes of H₂O, non-H-bonded structures of NH₃ with F₂ and CO₂ are strongly favored, with, in the latter case, no H-bonded minimum existing. In the complexes of CO there is, in addition to the competition between H-bonded and non-H-bonded structures, the competition between C...H and O...H H-bonded structures, which is always won by the C...H isomer due to significantly stronger σ -donor ability of the carbon lone pair.⁴⁸

3. Complexes of Rare Gases with BeO

Stable molecules involving the rare gases xenon and krypton have been known since 1963,⁶⁹ but corresponding molecules involving helium, neon, and argon have not yet been observed, other than very weakly bound van der Waals complexes.⁷⁰ Recently, however, some more strongly bound species have been discovered calculationally, involving the bonding partner BeO.⁷¹ Rare gases are of course very poor acceptors, but can serve as donors in complexes with BeO, which is a strong acceptor through its σ^* _{BeO} orbital. The work of Koch et al.⁷¹ has been extended by Hobza and Schley-

er,⁷² who employed basis sets that exhibited less basis set superposition error. The latter workers also performed NBO analysis and confirmed that the essential nature of the interaction is charge transfer. At the MP2 level, using extended basis sets, they found binding energies for HeBeO, NeBeO, and ArBeO of 4.8, 4.8, and 10.1 kcal/mol, respectively. In the case of HeBeO, for example, ΔE_{CT} is found to be -24 kcal/mol in the He → BeO direction, and -3.7 kcal/mol in the reverse direction. The overlap (see section II.C) of the donor 1s orbital of He with the acceptor σ^* orbital of BeO was found to be quite large, at 0.42. Dispersion is not important in these complexes, as the MP2 binding energies are only 0.3–0.6 kcal/mol greater than the SCF values. It is surprising that He bonds as strongly to BeO as does Ne; this is due to the stronger orbital overlap in the He case, and the fact that some back-transfer to He is possible (the lowest unoccupied orbital of He is much lower than that of Ne or Ar).

C. Ion-Molecule Complexes and Contact Ion Pairs

1. Anion-Water Complexes

The interaction between ions and neutral molecules has generally been interpreted as being electrostatic in nature.^{73,74} Kebarle,⁷³ referring to the fact that only 0.05 e was transferred from F⁻ to H₂O in the F⁻:H₂O complex (binding energy 23.3 kcal/mol), concluded that the hydrogen bond was “essentially electrostatic in nature”. However, NBO analysis has indicated that transfers of small quantities of charge (0.01 e or less) can correspond to energy changes (\approx 0.01 au) that are chemically very significant and that charge transfer can play a dominant role in H-bonded complexes involving neutral molecules (see section III.A.4).

In anionic H-bonded complexes, the role of purely electrostatic (particularly, ion-dipole) interactions is enhanced, but the CT interactions are also expected to increase due to the increased donor strength of the anion. Since the CT interactions increase exponentially with interpenetration of the van der Waals spheres and are highly sensitive to orbital shape, they may exert a disproportionate influence on the short-range energetics and geometries of cluster ions. Table VI presents NBO estimates of ΔE_{CT} , the changes $\Delta E_{\text{A} \rightarrow \text{B}}$ and $\Delta E_{\text{B} \rightarrow \text{A}}$ in the individual molecular directions, and the net charge q transferred between monomers for a number of anion-molecule complexes involving hydrogen bonding. As can be seen from Table VI, the CT contributions for the anion complexes are of the same general magnitude (-11 to -34 kcal/mol) as ΔE . As expected, charge

transfer is found to occur almost exclusively in the ion → molecule direction. The role of charge transfer in the structural features of the $\text{O}_2^- \cdot \text{H}_2\text{O}$ complex is significant and has been described in detail in ref 75. However, the ΔE_{CT} for the anion complexes are not dominant as in the case of neutral hydrogen-bonded complexes (see Figures 6 and 7). Thus, without significant electrostatic contribution, ΔE_{CT} would not be large enough to give rise to the net ΔE , as well as overcome the strong steric repulsions that must be present at the close approach distances of these anion-molecule complexes. It should be noted that even though ΔE_{CT} does not dominate in these hydrogen-bonded anion-molecule complexes, it is as large as, or larger than, that of the neutral hydrogen-bonded complexes.

2. Cation-Water Complexes

The situation is significantly different in the case of the cation-water complexes. Such complexes do not involve hydrogen bonding. The NBO estimates of the charge transfer in a series of cation-water complexes (cation = Li^+ , Na^+ , Mg^{2+} , Fe^{2+} , Fe^{3+}) are listed in Table VI. The ΔE_{CT} values are only 5–40% of the ΔE values. This is a significantly smaller proportion than for the anion-water complexes. The reduced importance of ΔE_{CT} for the cation-water complexes is due to the fact that the metal cations are poor acceptors compared to the H_2O σ^* orbitals, which accept most of the charge in the anion-water complexes. However, it appears that the charge transfer is significantly larger in the transition metal cation-water complexes than in alkali metal or alkaline earth complexes.

Whereas NBO analysis presents a picture of the bonding in these ion-molecule complexes that is generally in accord with chemical intuition, there are sharply contrasting results for ion-water complexes from analyses by Morokuma-type SCF partitioning.⁷⁴ As expected (see section IV.B), a Morokuma-type analysis gives the electrostatic interaction as the predominant attractive force. However, the Morokuma-type charge-transfer component is calculated to be positive, the values for Li^+ , Mg^{2+} , and F^- complexes with H_2O being +5.2, +108, and +7.2 kcal/mol, respectively. This is contrary to physical intuition and, hence, is referred to as a “residual” energy containing higher order effects.⁷⁴

Finally, as mentioned in section III.A.5, cooperativity effects in cluster formation seem to be generally associated with donor-acceptor interactions. In cases where a monomer can participate concertedly as a donor and acceptor (as in the case of neutral water clusters), the binding tends to be cooperative. In cases where a species must participate as a *multiple* donor (as in the anion complexes) or acceptor (as in the case of cation complexes), the binding is not cooperative. There are numerous examples of this in the literature.^{66,75,76}

3. Bifluoride Ion

A special case of ion-molecule H-bonding is the bifluoride ion FHF^- . Here, the donor-acceptor interaction is so great that the donor F^- and the F atom of the HF acceptor become indistinguishable; one has a symmetric structure where hydrogen is effectively hypervalent (bivalent). This limiting case of extremely strong

H-bonding was investigated by a calculation at the HF/6-31G* level on FHF^- ,⁴¹ using F-H bond lengths (1.13 Å) that are in accord with the range of F-F distances found in crystals (2.26–2.28 Å).⁷⁷ The NBO analysis leads to one of two equivalent Lewis structures: $\text{F}^- \cdots \text{H}-\text{F}$ or $\text{F}-\text{H} \cdots \text{F}^-$. The departure from the Lewis structure is very large: the $n \rightarrow \sigma^*_{\text{HF}}$ CT interaction amounts to 0.20 e and about 160 kcal/mol in magnitude.⁴¹ The H-F bond is *very* polar (88.9% toward F, compared to 77.8% in HF), and thus the antibond is practically a hydrogen 1s orbital (σ^*_{HF} is polarized 88.9% toward H). This species provides a dramatic example of Bent's rule.³³ The hybridization on fluorine of the H-F bond orbital is 31.8% s character in FHF^- , compared to 20.7% s character in isolated HF, so that the polarization and s character both increase by about 11% upon complexation with fluoride. The natural charges are rather ionic: -0.80 on F and +0.60 on H. A fully ionic model of this species, $[\text{F}^-][\text{H}^+][\text{F}^-]$, strongly modified by donor-acceptor interactions of the order of 0.20 e, is equivalent to Pimentel's three-center, four-electron MO bonding model of this system.⁷⁸ It is interesting to note that the electron population on H (0.4 e in this case) will be twice the amount of each $\text{F}^- \rightarrow \text{H}^+$ donor-acceptor interaction in the ionic model. Note also that the value (0.20 e) of $n \rightarrow \sigma^*$ CT in the structure $\text{F}^- \cdots \text{H}-\text{F}$ is that which is needed to make the electron distribution of this structure equivalent to that in the alternative resonance structure, $\text{F}-\text{H} \cdots \text{F}^-$. This system should be compared with benzene, where the amount of $\pi \rightarrow \pi^*$ CT out of each π bond that is needed to convert from one resonance structure to the other is 0.33 e.⁴¹

4. “Salt” Isomer of Carbon Tetrachloride

The possibility of non-H-bonded $n \rightarrow \sigma^*$ interactions has been suggested by Weiss, primarily in connection with experimental studies of iodocarbenium iodide species of type $\text{R}_2\text{C}^+ \cdots \text{I}^- \cdots \text{I}^-$.⁷⁹ Weiss pointed out that an analogous species, trichlorocarbenium chloride, $\text{Cl}_2\text{C}^+ \cdots \text{Cl}^- \cdots \text{Cl}^-$, might have transient stability and that this could be a possible structure for the $\text{CCl}_3^+ \cdots \text{Cl}^-$ ion-pair species that Bühl and Hurni have postulated to explain the transient 500-nm absorption observed in pulse radiolysis studies of liquid CCl_4 .⁸⁰ The apparent stability of such a “salt” isomer of carbon tetrachloride of C_{2v} symmetry was confirmed by high-level ab initio calculations,⁸¹ leading to the conclusion that the $n(\text{Cl}^-) \rightarrow \sigma^*(\text{C}-\text{Cl})$ CT stabilization is of the order of 30 kcal/mol. Changes in the forms of the NBOs analogous to those discussed previously in the water dimer were found to occur. Though this ion pair is primarily stabilized by the ionic interaction, the additional $n \rightarrow \sigma^*$ interaction is needed to make this unusual isomer of carbon tetrachloride a minimum on the potential energy surface. A number of important factors will tend to make a salt isomer of carbon tetrachloride significantly more favorable than that of carbon tetrachloride, including the fact that $\sigma^*(\text{C}-\text{I})$ will be a better acceptor than $\sigma^*(\text{C}-\text{Cl})$.

5. Ground and Excited States of $(\text{CO})_2^+$

Gas-phase dimer cations $(\text{XY})_2^+$ are species of atmospheric interest whose typical bond energies of ~ 1

eV are somewhat stronger than those of van der Waals complexes and hydrogen-bonded species, yet much weaker than typical chemical bonds. The $(CO)_2^+$ ion is highly anomalous among such species in that its photodissociation spectrum is found to consist of well-resolved vibrational bands in the near-UV⁸² [rather than the broad, featureless continuum absorption that characterizes other simple $(XY)_2^+$ species, including isoelectronic $(N_2)_2^+$]⁸³. Ab initio MCSCF methods and NBO analysis have been used to explore the ground 2B_u and excited 2B_g and 2A_g potential energy surfaces of this interesting species.^{84,85}

NBO analysis of $(CO)_2^+$ in terms of its parent CO and CO^+ monomers reveals that the surprising topological features of the ground potential energy surface can be associated with an avoided crossing between two "adiabatic" potential surfaces of quite different electronic character, dividing the surface into two distinct regions. The "outer" region corresponds to the usual weakly bound state that correlates to ground-state $CO + CO^+$ fragments, while the "inner" region corresponds to a covalently bonded carbon suboxide structure that correlates to an excited-state asymptote $CO(\tilde{A}^1\Pi) + CO^+$. These regions are connected by a low-energy, nonlinear valley that permits remarkably large geometry changes (e.g., $\sim 0.9\text{-}\text{\AA}$ CC stretches, $\sim 70^\circ \angle_{CC}$ bends with only about 15 kcal/mol excitation energy). The "weakly bound" $(CO)_2^+$ is thus found to be a species of ambivalent electronic structure, a remarkably short equilibrium bond distance ($R_{CC} \approx 1.5\text{\AA}$, about half the van der Waals contact distance), a pliable nonrigid structure, and complex vibrational dynamics.

Reference 84 describes how NBO analysis was used to provide qualitative pictures of the dimer ion states evolving from monomer fragment states and to show how a qualitatively simple picture can be useful in electronically complicated open-shell species such as $(CO)_2^+$. The NBO procedure leads to strikingly different orbitals for α and β spins in the open-shell species CO^+ and $(CO)_2^+$, indicative of the need for "different Lewis structures for different spins"¹³ to describe these structures compactly.

A noteworthy feature of the analysis is the need to treat both the outer limit of weak van der Waals bonding and the inner limit of strong covalent bonding (where an electrostatic treatment would be manifestly inadequate). NBO analysis of $(CO)_2^+$ shows clearly the continuity between these two limits and how the weak donor-acceptor character of the outer limit (the n_C lone pair of CO donating into the half-occupied n_c of CO^+) merges smoothly into the covalently bonded inner limit via a "banana-bonded" bent intermediate. Thus, this system serves to demonstrate the close connection between the van der Waals bonding regime and the regime of covalent phenomena, and to show how the NBO donor-acceptor picture can illuminate interesting *chemical* aspects of the bonding that are intrinsically beyond electrostatic models.

D. Chemisorption

The traditional picture of bonding of lone-pair ligands to metals is based on σ donation to the metal and π donation from the metal to the ligand.^{86,87} For CO bonding to metals, the σ donation arises from the $5s$ molecular orbital of CO to the unoccupied metal σ or-

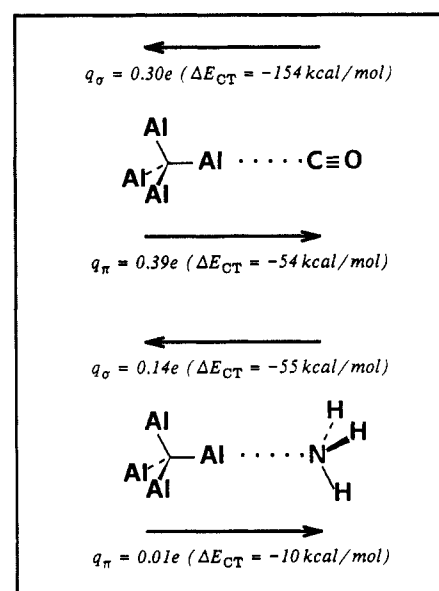


Figure 10. Summary of natural population changes (and associated energy lowerings ΔE_{CT}) for $Al_4\cdots CO$ and $Al_4\cdots NH_3$ complexes (UHF/3-21G level), showing the σ donation (q_σ) and π back-donation (q_π) that accompany formation of each complex.

bitals; the π donation is from the metal to the empty ligand orbitals ($2\pi^*$ MO) of CO. This picture of the bonding also holds for the bonding of CO to metal surfaces.⁸⁸⁻⁹⁰

The natural bond orbital method strongly supports this traditional picture in calculations on $Al_4\cdots CO$ and $Al_4\cdots NH_3$.⁹¹ These calculations were done with CO and NH_3 sitting atop an Al_4 tetrahedral cluster (spin triplet). The results from a 3-21G calculation⁹¹ are summarized in Figure 10. The nature and extent of the orbital interaction between Al_4 and CO or NH_3 can be judged by comparing the forms and occupancies of the NBOs in the isolated species with those in the complex. The most significant occupancy changes in $Al_4\cdots CO$ are a depletion of the carbon lone pair NBO by 0.30 e, with an associated occupancy increase of NBOs of σ symmetry on Al_4 , and an increase of 0.39 e in the occupancy of the CO π^* NBOs, with an associated depletion of the Al_4 total π occupancy. However, the π^* back-transfer occurs only in the α -spin manifold as there are no occupied valence orbitals on Al_4 of π symmetry in the β -spin manifold. Since occupancy changes of other NBOs are minor (<0.01 e) in comparison to these, the cited NBO occupancy changes can be used to decompose the net charge transfer of 0.09 e determined by NPA in σ and π components, q_σ and q_π , as given in Figure 10. In the $Al_4\cdots NH_3$ complex, where π^* back-transfer is not possible, the net CT of 0.14 e from NH_3 to Al_4 is almost entirely accounted for by the occupancy loss of the nitrogen lone pair NBO. A significant amount of nonadditivity in ΔE_{CT} is observed. This is due to the fact that the total CT energy is quite large (-175 and -74 kcal/mol in $Al_4\cdots CO$ and $Al_4\cdots NH_3$, respectively), and the CT interaction is thus a very strong perturbation on the system. In the other complexes in this review, the ΔE_{CT} values were much smaller in magnitude and no significant nonadditivity was observed.

The bonding in the $Al_4\cdots CO$ system is quite interesting in that very large changes in the electronic structure of CO occur even though the binding energy

of the complex (i.e., the driving force for these changes) is only a couple of kcal/mol. The strong CT interactions are thus almost equally balanced by strong repulsive interactions (the Al-C distance is only 1.98 Å, much closer than van der Waals contact) and the metal-CO bond is relatively labile. Note that the binding strength is on the same order as that in the water dimer, a complex where much smaller changes in the electronic structure occur. The bonding of CO with Al₄ is also closely related to the bonding of CO with HF (section III.A.2) and with CO⁺ (section III.C.5), the major differences being the strength of the CT interaction and the additional feature of π^* back-transfer.

Bagus et al.^{92,93} have come to a contrary conclusion using CSOV analysis,⁹⁴ an analysis method of Morokuma type (section IV.B).^{95,96} For example, the CO σ donation to Al₄ in the Al₄...CO complex is calculated in CSOV analysis to contribute only 9.5 kcal/mol to the binding energy, as opposed to around 150 kcal/mol in the NBO analysis. The unsymmetrical treatment of valence-space intermolecular overlap in the Csov method, the unoccupied orbitals of one monomer (e.g., the valence-space σ -accepting orbitals of Al₄) being implicitly Schmidt orthogonalized to the occupied orbitals of the other monomer (e.g., the carbon lone pair of CO), has the consequence that the portion of the intermolecular stabilization energy directly associated with valence-shell intermolecular overlap is absorbed into electrostatic energy terms. Charge transfer and delocalization are, of course, not strictly definable in quantum mechanics and thus the Morokuma-like Csov analysis has its own mathematical validity, given the particular definitions of the various energy decomposition terms that it employs. However, in orbital models in chemistry, one usually associates strong valence-shell intermolecular (or intramolecular) overlap with strong delocalization effects. By effectively absorbing such terms (via Schmidt orthogonalization) in localized "electrostatic" contributions, Csov analysis deemphasizes this aspect of the bonding. The symmetric treatment of valence-shell overlap in the NBO procedure is thus much more consistent with the commonly used orbital interaction models (section IV.B). The strong σ -donor role of CO has also been confirmed in a recent GVB study on Ni₃Al-CO by Tatar and Messmer.⁹⁷ The buildup of partial metal-carbon σ bonding is clearly seen in their orbital plots, as well as a significant amount of π^* _{CO} back-bonding.

E. Relationships between Inter- and Intramolecular Interactions

When a bond (and antibond) involves a multivalent and a monovalent element (such as C-F or O-H), one can speak of it as having "inward" and "outward" ends with respect to the molecule. We wish to point out here the relationship of the outward (intermolecular) $n \rightarrow \sigma^*$ interactions discussed so far with inward (intramolecular) $n \rightarrow \sigma^*$ and $\sigma \rightarrow \sigma^*$ interactions, which are more commonly referred to as hyperconjugation or negative hyperconjugation. This allows intra- and intermolecular interactions to be discussed on a common footing.

One of the first applications of bond orbital analysis was to the study of the internal rotation barrier of ethane.⁹⁸ It was found that the rotation barrier prac-

tically disappears⁹⁸ or is reversed in sign^{41,99} upon removal of the σ^*_{CH} orbitals from the basis set. The rotation barrier can thus be attributed to $\sigma \rightarrow \sigma^*$ hyperconjugation.¹⁰⁰ (Other interpretations of the rotation barrier of ethane are mentioned in section IV.B.) The $\sigma \rightarrow \sigma^*$ interaction was found to be increased when the accepting antibond was made more polar (i.e., σ^*_{CF}) and decreased when the donor bond was made more polar (i.e., σ_{CF}). Replacement of the σ donor with a lone pair donor n significantly increases the interaction with the σ^* orbital. Such $n \rightarrow \sigma^*$ interactions constitute negative hyperconjugation.¹⁰¹ The involvement of negative hyperconjugation in the generalized anomeric effect¹⁰² has recently been confirmed through detailed natural bond orbital analysis studies.¹⁰³ The generalized anomeric effect involves the preferential stabilization of conformations of R_nY-AH_m-X species where the lone pair of highest p character on the donor atom Y is antiperiplanar to the acceptor σ^*_{AX} orbital, X being an element significantly more electronegative than the central atom A.¹⁰¹⁻¹⁰³ Negative hyperconjugation of $n_{\text{N}} \rightarrow \sigma^*_{\text{AF}}$ type (analogous to hydrogen bonding of $n_{\text{N}} \rightarrow \sigma^*_{\text{HF}}$ type) is found to be particularly strong, leading to, for instance, a rotation barrier of 18 kcal/mol in FSNH₂.^{103b}

A topic of particular interest with respect to this review is the coupling between intra- and intermolecular charge transfer. The influence of solvent on the anomeric effect is, for example, a topic of current interest in the literature.¹⁰⁴ In a recent study of coupling between hydrogen bonding and negative hyperconjugation, we optimized structures for various complexes of CISNH₂ with HF.^{103d} The anomeric effect is particularly strong in the case of CISNH₂, which exhibits a single minimum for the syn conformation.^{103b} On going from the syn minimum to the transition state for internal rotation of uncomplexed CISNH₂, the changes in the energy, S-N and S-Cl bond lengths, and sum of the bond angles at N ($\sum \theta_{\text{N}}$) are found (at the HF/6-31G* level) to be $\Delta E = +15.9$ kcal/mol, $\Delta R(\text{S}-\text{N}) = +0.104$ Å, $\Delta R(\text{S}-\text{Cl}) = -0.048$ Å, and $\Delta \sum \theta_{\text{N}} = -26.7^\circ$. This is consistent with the strong $n_{\text{N}} \rightarrow \sigma^*_{\text{SCl}}$ interaction seen in the NBO analysis, which favors a significant planarization at nitrogen in the syn conformer (consequently, there is no minimum for the anti conformer of CISNH₂).^{103b} The results of full geometry optimization of complexes of CISNH₂ with HF are summarized in Table VII.^{103d} Complexation of HF to the nitrogen lone pair in an N...HF manner reduces the energy and geometry changes upon internal rotation to $\Delta E = +12.2$ kcal/mol, $\Delta R(\text{S}-\text{N}) = +0.080$ Å, $\Delta R(\text{S}-\text{Cl}) = -0.031$ Å, and $\Delta \sum \theta_{\text{N}} = -18.4^\circ$. This is because the nitrogen lone pair must now donate in two directions. Complexation of HF to the chlorine in a Cl...HF fashion [$\theta(\text{S}-\text{Cl} \cdots \text{H}) \sim 105^\circ$] results on the contrary in increased energy and geometry changes upon internal rotation: $\Delta E = +17.0$ kcal/mol, $\Delta R(\text{S}-\text{N}) = +0.111$ Å, $\Delta R(\text{S}-\text{Cl}) = -0.058$ Å, and $\Delta \sum \theta_{\text{N}} = -28.9^\circ$. Here, a positive cooperativity effect is observed, the electron acceptor HF acting to encourage stronger hyperconjugation from the nitrogen lone pair. The changes in the internal rotation barriers are of course due to differing strengths of hydrogen bonding in the syn and transition structures. The hydrogen bond formed by HF with the nitrogen lone pair, for instance, has a strength of only -5.2 kcal/mol with the syn structure, but -8.9 kcal/mol with the transition structure. The latter value is much closer to the

TABLE VII. Relative Energies (kcal mol⁻¹) and Key Geometrical Parameters (Å, Degrees) of Hydrogen-Bonded Complexes of HF with CISNH₂ from Full HF/6-31G* Optimizations^a

species	<i>E</i> (H bond)	<i>E</i> _{rel}	<i>R</i> (H bond)	<i>R</i> (S-N)	<i>R</i> (S-Cl)	<i>θ</i> (NSCl)	$\sum\theta_N$
Minimum Structure with CISNH ₂ in Syn Conformation (<i>C</i> _s)							
CISNH ₂ + HF	0.0	0.0	∞	1.642	2.074	105.8	346.7
CISNH ₂ ...HF	-5.2	-5.2	1.98	1.670	2.052	104.3	339.5
FH...CISNH ₂	-2.4	-2.4	2.57	1.633	2.092	105.5	349.1
Transition Structure for Internal Rotation about S-N Bond (<i>C</i> ₁)							
CISNH ₂ + HF	0.0	+15.9	∞	1.746	2.026	99.5	320.0
CISNH ₂ ...HF	-8.9	+7.0	1.88	1.750	2.021	99.3	321.1
FH...CISNH ₂	-1.3	+14.6	2.70	1.744	2.034	99.2	320.2

^a Data from ref 103b; $\sum\theta_N$ is the sum of the HNH and the two SNH angles, and *R*(H bond) is the distance of the hydrogen bond with HF. Energies are all relative to isolated syn CISNH₂ and HF.

HF/6-31G* energy of the H₃N...HF bond of -12.2 kcal/mol. If an HF molecule bonds to both the chlorine and nitrogen sites of CISNH₂, one can estimate from these results that the internal rotational barrier would undergo a net reduction of 2.6 kcal/mol from the isolated-molecule value. Without the donor-acceptor model of the anomeric effect and of the hydrogen bond, such changes would be more difficult to rationalize in chemical terms.

Intramolecular vibrational excitation can directly affect the strength of both intra- and intermolecular forces. The case of vibrationally excited A-H bonds is of particular experimental interest, since hydride bonds characteristically exhibit the large anharmonicities that make it feasible to selectively excite high-*v* states by laser overtone spectroscopy.¹⁰⁵ It is easy to recognize from the donor-acceptor picture that elongation of an A-H bond through vibrational excitation should generally increase the acceptor strength of the associated σ^*_{AH} hydride antibond, making it a better Lewis acid.¹⁰⁶ Overtone excitation of an A-H stretch should thus tend to strengthen hyperconjugative interactions involving the σ^*_{AH} orbital, including hydrogen bonds. In the case of intramolecular interactions of rotation barrier type, particularly strong effects of this type have been observed as vibration-torsion coupling terms in high-overtone states of hydrogen peroxide, as investigated experimentally by Dübal and Crim,¹⁰⁷ and high-level ab initio calculations and NBO analysis have led to a very satisfactory qualitative and quantitative account of the theoretical origin of these effects.³⁹ In the case of intermolecular interactions of H-bond type, related effects of vibrational excitation (likely to have a similar origin) have been observed in high-precision nozzle-beam vibrational spectroscopic studies of van der Waals complexes by Nesbitt and co-workers.¹⁰⁸

Coupling between inter- and intramolecular donor-acceptor interactions is of enormous biological importance, for the intermolecular interactions between functional groups on enzymes and substrates at active sites induce *intramolecular* changes that enhance and direct substrate reactivity. Specifically directed intermolecular interactions can thus serve catalytic functions through their donor-acceptor character (as well as in other ways). Further discussion of this topic (cf. sections III.A.5 and III.A.6) is beyond the scope of this review, and the reader is referred to the reviews of Kirby, of Deslongchamps, and of Gorenstein.¹⁰² Intermolecular donor-acceptor interactions are biologically important not only with respect to stereoelectronic acceleration of enzymatic reactions but also with respect

to the mechanisms of molecular binding and recognition.

IV. Relationship of Donor-Acceptor and Electrostatic Models

A. Historical Overview

As pointed out in the Introduction, the van der Waals bonding regime lies at the interface between "chemical" and "physical" bonding. Historically, therefore, it has been interpreted in terms of varying proportions of interactions of chemical (donor-acceptor) and physical (electrostatic, polarization, dispersion) nature.¹⁰⁹ In this section, we shall discuss in detail the relationship of donor-acceptor and electrostatic models of van der Waals complexes, with emphasis again on the hydrogen bond.

With regard to the first theoretical conception of the hydrogen bond, it is appropriate to cite Lewis's 1923 book on valence theory.¹¹² In a section with the provocative title "Bivalent Hydrogen", Lewis wrote, "It seems to me that the most important addition to my theory of valence lies in the suggestion of what has become known as the hydrogen bond. The idea was first suggested by Dr. M. L. Huggins, and was also advanced by Latimer and Rodebush [ref 113]... This suggestion is that an atom of hydrogen may at times be attached to two electron pairs of two different atoms, thus acting as a loose bond between these atoms." Lewis dot structures for the water dimer and the bi-fluoride ion FHF⁻ were drawn,^{112,113} and Lewis suggested the use by hydrogen of a secondary valence shell. This initial discussion, of course, preceded the introduction of quantum mechanics. Thereafter, Pauling argued on the basis of the Pauli exclusion principle and the fact that the hydrogen atom has only one valence orbital that hydrogen bond formation must be due to ionic forces.¹¹⁴ The success of simple electrostatic models in predicting the hydrogen bond energy between water molecules was then generally taken as proof of the essentially electrostatic nature of the hydrogen bond. The 1960 book by Pimental and McClellan¹¹⁵ represented a departure from this line of thought. They wrote, "At the 1957 Ljubljana Conference one of the important points of fairly general accord was that the electrostatic model does not account for all of the phenomena associated with H bond formation." They tended to favor a more covalent description of the hydrogen bond, though they realized the difficulty of

reconciling extravacency with covalent bonding concepts. In this book, Pimentel's MO description^{78,116} of the symmetric trihalide and bifluoride ions (three-center, four-electron bonding model) was extended to unsymmetrical hydrogen bonds. Many workers still preferred an electrostatic model, however.

The discussion up to this point had been based out of necessity on crude (though intelligently chosen) wave functions for hydrogen-bonded systems, as exemplified by the valence bond analysis of Coulson,¹¹⁷ and one might have expected that the controversy would be resolved with the rapid improvement of computers and of quantum chemical methods in the 1960s and 1970s. Indeed, when taken at face value, the influential work of the Kollman¹¹⁸ and Morokuma¹¹⁹ groups in the 1970s would seem to have resolved the controversy in favor of electrostatics.¹²⁰ The present decade has witnessed the (in many respects successful) modeling of solutions and biological molecules, and this has been achieved to a large extent through the adjustment and application of electrostatic potentials.¹²¹ In addition, Buckingham and co-workers¹²² have recently developed a rather successful electrostatic plus hard-spheres repulsion model of van der Waals complexes. It would seem, therefore, that a solid body of theoretical evidence against a donor-acceptor model of hydrogen bonding exists. These conclusions have been disputed, however, by Klemperer and co-workers, who have favored donor-acceptor models for the structures of many of the van der Waals complexes that they have studied experimentally.¹²³ As we shall discuss, we believe that the evidence that has been put forth against the donor-acceptor model rests more on the assumptions embedded in the analysis methods than on the wave functions themselves and that NBO analysis permits modern calculations to be essentially reconciled with the conceptions expressed by Lewis, Coulson, Pimentel, Klemperer, and others.

B. Relationship to Kitaura-Morokuma Analysis

The most widely applied method for decomposing ab initio intermolecular interaction energies is that of Kitaura and Morokuma (KM).⁹⁵ In the case of the water dimer, for instance, the ΔE_{CT} estimates by the KM and NBO methods are -1.8^{96} and -9.6^{45} kcal/mol, respectively, at the 6-31G** basis set level. According to KM analysis, the electrostatic energy term plays the central role in the hydrogen bond,⁹⁶ in contrast to the central role of charge transfer that is assigned by NBO analysis. This qualitative discrepancy in the analyses has its subtle origin in the treatment of the valence-shell intermolecular overlap, or, roughly said, in how one "draws the line" between the two molecules in the valence-shell orbital space.

In order to define charge transfer, one first partitions the total AO space into orthogonal subspaces associated with each species, so that electron occupancy can be divided between them. (We restrict our discussion to the valence-shell AO space, as the core and extra-valence-shell AO spaces are of little importance in terms of the intermolecular interaction energy.) In the NBO procedure, this is done explicitly by the weighted symmetric orthogonalization procedure, incorporating all valence NAOs (the natural minimal basis, NMB; section II.A) of each atom in the dimer. When the orthonormal

NAOs are transformed to orthonormal NBOs, the space spanned by the nearly doubly occupied lone pair and bond (in-phase) orbitals *plus that spanned by the corresponding antibonds* is nearly equivalent to the space that is spanned by the NMB (see section II), which is the valence-shell space of the constituent atoms.

In contrast, the partitioning of the AO space in the KM decomposition is carried out implicitly, based on the antisymmetrization of the product of nonorthogonal occupied MOs. In effect, the virtual MO space of each monomer is Schmidt orthogonalized to the occupied MO space of the other monomer. (In the closely related method of Stevens and Fink,¹²⁴ the Schmidt orthogonalization is carried out *explicitly*, and the numerical results are very similar to KM analysis.) Since the antibonds have low occupancy, they will be almost entirely contained in the virtual monomer MO space. To illustrate this, consider the overlap of the proximate oxygen lone pair orbital (which is almost entirely contained in the occupied MO space due to its near double occupancy) with the O-H antibond orbital in the water dimer. After the implicit Schmidt orthogonalization, almost all of the $n \rightarrow \sigma^*$ overlap has been awarded to the oxygen lone pair, so that it significantly penetrates the region around the acceptor monomer. Most of the energy associated with the proximate $n \rightarrow \sigma^*$ overlap is therefore attributed to energy terms involving occupied orbitals only. As will become more obvious from the discussion below, the $n \rightarrow \sigma^*$ energy term is incorporated in the electrostatic interaction energy term. It is then clear that the KM decompositon must consistently lead to a much smaller estimate of charge transfer, since the only contribution attributed to unfilled (acceptor) orbitals is from remnant portions of these orbitals having no significant overlap with filled orbitals. But since both the filled n and unfilled σ^* orbitals originate from the atomic valence shells, this procedure amounts to a highly unsymmetric orthogonalization of the atomic valence subspaces. In effect, the KM procedure employs symmetric orthogonalization for only 8 of the 12 valence AOs of the water dimer, whereas the remaining *one-third* of the valence AO space is subjected to Schmidt orthogonalization. The KM method thus involves an unsymmetrical treatment of the valence AO space, which necessarily implies some loss of resemblance to parent nonorthogonal AOs in the sense of Löwdin's maximum resemblance theorem (section II.A).

NBO analysis^{8,45} stresses the role of quantum mechanical orbital interaction of filled and unfilled orbitals, whereas the KM analysis stresses the role of classical electrostatics of overlapping charge distributions. When two molecules are brought together, the orbitals of each monomer penetrate into the regions of Cartesian space that are occupied by the positively charged nuclei of the other molecule. This leads to a lowering of the potential energy of the valence AOs of each monomer by virtue of the increased electron-nuclear attraction. [It is important to mention that, as two spherically symmetric (unpolarized) atoms such as He are brought together, the electron-nuclear attraction increases faster in magnitude than the sum of electron-electron and nuclear-nuclear repulsion.¹²⁵ For this reason, there is a *net* electrostatic attraction between any pair of molecules when the Pauli exclusion repul-

sion is ignored.] A large part of this energy lowering is artificial, however, for the valence orbitals of each monomer are penetrating into regions of the valence (and core) orbitals of the other monomer without the corresponding increase in kinetic energy that is required by the Pauli exclusion principle. This penetration is avoided in the NBO method, because the "orthogonalization tails" at other nuclei incorporate the kinetic energy increase needed to prevent the Pauli-violating delocalization of the valence AOs of one monomer into those of the other. The valence AOs of each monomer are thereby raised in energy and reduced in "volume" to values consistent with their actual molecular environment.²³

The first step of the KM analysis involves computing the wave functions ψ_A and ψ_B of the isolated monomers A and B and then bringing the monomers together to their position in the complex without allowing the wave functions to change.⁹⁵ This is accomplished through the *exclusion-principle-violating* wave function ψ_{ES} , from which the KM electrostatic interaction energy is defined:

$$\psi_{ES} = \psi_A \psi_B \quad (20)$$

$$\Delta E_{ES} = E(\psi_{ES}) - E(\psi_A) - E(\psi_B) \quad (21)$$

Pauli exclusion is restored through the action of the antisymmetrizer \mathcal{A} on ψ_{ES} , leading to the KM definition of the exchange interaction energy:

$$\psi_{EX} = \mathcal{A}\psi_{ES} \quad (22)$$

$$\Delta E_{EX} = E(\psi_{EX}) - E(\psi_{ES}) \quad (23)$$

The antisymmetrizer \mathcal{A} in eq 23 corrects for the penetration of the electrons of monomer A into the regions of orbital space of the *occupied* orbitals of monomer B, but not for the penetration of the monomer A electrons into the regions of the unoccupied orbital space of the valence-shell orbitals of monomer B involving the antibonds. Terms corresponding to the overlap of filled orbitals of one monomer with unfilled orbitals of the other thus remain embedded in the wave function $\mathcal{A}\psi_{ES}$ and are therefore defined as "electrostatic" in nature. Only the energy changes *beyond* those incorporated in $\mathcal{A}\psi_{ES}$ (and thus, involving only those portions of unfilled monomer orbitals that are orthogonal to filled orbitals on the other monomer) are defined as being of "charge-transfer" type.

It is apparent from this discussion, however, that no *a priori* argument in favor of the NBO or the KM decomposition can be made on the basis of quantum mechanics, and whichever description one prefers will depend on how one defines the words "electrostatic", "charge transfer", "delocalization", etc. Since the molecular Hamiltonian contains only Coulombic potential terms (and is in this sense purely electrostatic in nature), there can be no ultimate conflict between NBO and "electrostatic" interpretation of the wave function. However, we believe that a satisfactory theory of H-bond complexes (with monomers lying 0.5 Å or more *inside* van der Waals contact) must be able to join smoothly with established concepts of covalency and coordinate covalency in the strong-overlap regime. In this respect the NBO donor-acceptor model has a significant conceptual advantage over electrostatic models.

Just as the concept of donor-acceptor interactions extends from inter- to intramolecular interactions and metal-ligand binding (sections III.D,E), so also does the controversy that surrounds it. The classic intramolecular case is that of the internal rotation barrier of ethane. In the framework of the NBO method, the rotation barrier is found to be due to $\sigma_{CH} \rightarrow \sigma^*_{CH}$ interactions, both at semiempirical⁹⁸ and ab initio^{41,99,100} levels of theory. Analysis by the Morokuma¹²⁶ and by Morokuma-like^{125,127} (in the treatment of valence-shell overlap)⁹⁸ methods leads to an exclusion repulsion explanation of the rotation barrier involving "filled" orbitals only.¹²⁸

A similar disagreement has arisen with regard to the origin of the anomeric effect.¹⁰² In NBO analysis, the anomeric effect is found to be due to $n \rightarrow \sigma^*$ negative hyperconjugation.¹⁰³ The Morokuma-like analysis method of Smits and Altona¹²⁵ characterizes the anomeric effect in terms of geminal exclusion repulsion interactions. The Smits-Altona method is based on *non-orthogonal* localized molecular orbitals. It is analogous to Morokuma analysis, the main difference being that, instead of starting with the nonorthogonal wave functions of two isolated monomers (or, two molecular fragments¹²⁶), one starts with the nonorthogonal localized molecular orbitals associated with *all* of the occupied core, lone-pair, and two-center bond orbitals of the molecule. Of course, all such interpretations based on nonorthogonal fragment orbitals are subject to the objection²³ (section II.A) that there can be no possible Hermitian Hamiltonian corresponding to the presumed initial energy E_i ; the calculated "energy change" $\Delta E = E_f - E_i$ therefore cannot have a meaningful physical interpretation.

As discussed in section III.D., the Morokuma-type analysis method that has been developed by Bagus et al.⁹²⁻⁹⁴ to analyze metal-ligand bonding and chemisorption to metal surfaces (CSOV analysis) leads to the conclusion that the traditional model of metal-CO bonding involving σ donation from the carbon lone pair to the metal is incorrect. NBO analysis of complexes of Al_4 with CO and NH_3 confirms the traditional σ -donor picture but also indicates the important role of π^* back-bonding interactions, as Bagus et al.⁹²⁻⁹⁴ have stressed.

C. Semiempirical Potential Functions

Up to now, intermolecular interactions have been primarily modeled in terms of electrostatics plus Lennard-Jones 6-12 potentials (the latter taking dispersion and exclusion interactions into account). This is partly due to the mathematical simplicity of Coulombic interactions and partly due to the widespread assumption that intermolecular interactions are primarily of electrostatic rather than donor-acceptor nature. It is clear from the discussion above that such electrostatic potential models can incorporate a significant portion of what is labeled charge-transfer energy in NBO analysis. The possibility of modeling intermolecular interactions with explicit inclusion of charge-transfer energy terms has not yet been seriously considered, though some of the available macromolecular modeling programs include an attractive "hydrogen bond" term that has an R^{-10} dependence.¹²⁹

Although a measure of success has been achieved by fitting classical electrostatic formulas to model H-bonding, such fits do not necessarily contradict the validity of the donor-acceptor picture.^{115,117} It is easy to recognize⁴⁵ how the n- σ^* interaction can be absorbed into an apparent "electrostatic" contribution by Schmidt-orthogonalizing the unfilled σ^* to the filled n orbital. The angular dependence of the n- σ^* interaction can often be mimicked by low-order multipole terms, since the n and σ orbitals are usually leading contributions to the dipole and quadrupole moments of a diatomic molecule. Spackman^{50b} has also pointed out that the electrostatic model assumption¹²² of zero van der Waals radius for the H atom is equivalent to neglect of steric repulsions (neglect of the Pauli principle¹²³) and neglect of an attractive charge-transfer interaction of approximately compensating strength.

Certain disadvantages of the electrostatic modeling approach can be mentioned. Such formulas are ill-adapted to describe H-bonding effects involving apolar species (such as CH₄; section III.A.6) which lack the leading terms of a multipole expansion. Since Coulomb's law involves pairwise-additive interactions only, classical electrostatic formulas are intrinsically incapable of describing cooperative effects (section III.A.5). Another aspect of the electrostatic potential approach is that the results are somewhat dependent on the choice of the dielectric parameter ϵ , which is often made to be distance dependent.¹³⁰ Also, reasonable results can be obtained without the use of electrostatic potentials, as shown by the recent work of Müller,¹³¹ who has developed a united atom force field method for polypeptides and other macromolecules that includes a special hydrogen bond function, but no Coulombic charges.

At the present time, the lack of empirical model potential functions based on the donor-acceptor approach must be counted a significant disadvantage, relative to the electrostatic approach. However, this situation also points to an opportunity for future work in this area to repair known defects of existing electrostatic model potentials with insights gained from the donor-acceptor picture.

V. Concluding Remarks

In this review, we have described the methodology of natural bond orbital (NBO) analysis and its recent applications to ab initio wave functions of "van der Waals molecules", particularly of H-bonded type. Our investigations have lent support to a *chemical* interpretation of the bonding in these species, based on orbital interactions of donor-acceptor (Lewis base-Lewis acid) type.

Although such a "charge-transfer" picture of hydrogen bonding had achieved considerable support in the decades preceding the advent of large-scale ab initio computer calculations in the 1960s, it came into apparent conflict with analyses of ab initio wave functions which suggested a relatively minor role for charge transfer.¹³² We believe that such interpretations rest on fallacious assumptions embedded in the analysis methods, rather than on the wave functions themselves. NBO analysis has shown how ab initio wave functions of the highest quality can be directly reconciled with

the simple donor-acceptor "chemical" picture. Such a chemical interpretation is in general harmony with the viewpoint expressed (among others) by Lewis, Coulson, Pimentel, and Klemperer, but it diverges sharply from the electrostatic view that has been espoused by many other workers.

What are the limits of the donor-acceptor picture? Clearly, charge transfer is unimportant in the weakest van der Waals molecules, such as He...He, where no empty valence-shell orbitals are available. As two He atoms are brought together, some charge transfer does indeed occur, but this is into high-energy (extravalence) 2s and 2p orbitals and is by no means strong enough to overcome the strong exchange repulsion of filled 1s orbitals. In this case, the equilibrium separation lies outside the distance of contact of empirical van der Waals radii, the overlap of filled orbitals is negligible, and the conditions for applying the standard theory of long-range intermolecular forces¹³³ are well satisfied. For donor-acceptor interactions to become important, the available acceptor orbitals must be sufficiently low in energy and must protrude further into space than the corresponding filled orbitals, as depicted in Figure 4. This allows the n- σ^* interaction to overcome n- σ repulsion and pull the monomers inside van der Waals contact distance. A criterion for significant donor-acceptor ("chemical", "overlap") character in the bonding is therefore that the van der Waals penetration distance d_p

$$d_p = R_{vdW} - R_{eq} \quad (24)$$

is appreciably positive, say, $d_p \geq 0.1 \text{ \AA}$. Since the empirical van der Waals radius is related to effective gas-phase collisional diameters under ambient conditions ($kT \approx 1 \text{ kcal/mol}$), one could also associate significant donor-acceptor character with complexes whose net binding energies are $\sim 1 \text{ kcal/mol}$ or higher. Such rough "rules of thumb" relating to d_p and D_e seem to do a good job in distinguishing complexes of donor-acceptor type (such as H-bonded complexes, clearly dominated by CT forces) from those where CT plays a secondary role to electrostatic and dispersion interactions (such as the T-shaped complexes of N₂ and O₂ with HF, H₂O, and NH₃).

In this context, it is instructive to characterize a van der Waals complex in terms of a dimensionless "covalency ratio" χ

$$\chi = \frac{R_{vdW} - R_{eq}}{R_{vdW} - R_{cov}} \quad (25)$$

where R_{cov} denotes the covalent bonding distance (sum of atomic covalent radii) for the atoms in closest contact in the complex. As the covalency ratio χ increases toward unity, the role of chemical overlap-type forces must become dominant, whereas for $\chi \rightarrow -\infty$, these forces are absent. Since the empirical van der Waals radius of an atom is approximately 0.8 Å greater than the covalent or metallic radius,¹³⁴ one can rewrite the expression for χ in the form

$$\chi \approx d_p / 1.6 \quad (26)$$

where d_p is in angstrom units. Common values of the covalency ratio for H-bonded species are in the neighborhood of $\chi \approx 0.3$, but range up to $\chi = 0.9$ for bi-

fluoride ion. It is highly implausible that overlap-type forces would have only a secondary role for all χ values in this range (as electrostatic models or the results of Morokuma-type analysis would suggest). Yet there is no apparent discontinuity in the properties of H-bonded complexes to suggest that the nature of the bonding changes abruptly in this range, nor any basis for exempting more strongly bonded species from Morokuma-type decompositions or electrostatic models as the results become increasingly implausible from a chemical point of view. NBO analysis suggests on the contrary that donor-acceptor interactions of $n \rightarrow \sigma^*$ type are the dominant, characteristic feature of the bonding throughout this range of χ values, and that the limiting "boundary" of the donor-acceptor model is near the value $\chi \approx 0\text{--}0.1$ of weak non-H-bonded complexes.

A distinguished theoretician once remarked,¹³⁵ "One of the principal objects of theoretical research in any department of knowledge is to find the point of view from which the subject appears in its greatest simplicity." In this golden age of discovery of van der Waals chemistry, the horizons of "the subject" are still expanding rather dramatically. There is reason to anticipate that studies of van der Waals molecules can lead to valuable insights into the solvation process as well as more general complexation phenomena such as host-guest interactions, biophysical self-assembly mechanisms, solvated electrons, Hassel compounds, etc.¹³⁶ As we strive to attain the point of view from which the rich structural and energetic patterns of van der Waals molecules appear in their greatest simplicity, we should also anticipate possible relationships to these more general chemical phenomena. At present, the donor-acceptor picture of van der Waals bonding remains a minority viewpoint.¹³⁷ However, we believe that as additional structures, patterns, and phenomena are encompassed within the term "van der Waals chemistry", the pervasive role of chemical (overlap type) interactions in complex formation will be more widely perceived, and the simplifications inherent in a unified donor-acceptor viewpoint will be increasingly appreciated.

Note Added in Proof. Since the completion of this manuscript, a number of additional NBO studies pertaining to donor-acceptor interactions have been carried out: Hydrogen bonding of solvated electrons to water clusters, ethanol, and propane [Reed, A. E.; Clark, T.; *J. Chem. Soc., Farad. Discuss.*, in press]; bonding in oligomers of methylolithium, and the influence of $\sigma_{\text{CH}} \rightarrow n_{\text{Li}}$ ("Li-H" or "agostic") interactions on the methyl group internal rotation barrier in the methylolithium tetramer [Kaufmann, E.; Raghavachari, K.; Reed, A. E.; Schleyer, P. v. R. *Organometallics*, in press]; the remarkable structures of salt-like ($\text{Al}^+\text{AlH}_4^-$) and Lewis acid/base ($\text{AlH}_3/\text{:AlH}$) structures of Al_2H_4 [Lammertsma, K.; Grüner, O. F.; Drewes, R. M.; Reed, A. E.; Schleyer, P. v. R. *Inorganic Chemistry*, in press]; the role of $\sigma_{\text{Si-Li}} \rightarrow n_{\text{Li}}$ delocalization ("Li-Li attraction") in the unusual C_{2v} structure of SiLi_4 [Schleyer, P. v. R.; Reed, A. E. *J. Am. Chem. Soc.* 1988, 110, 4453-4454]; a general overview of the NBO Lewis structure concept [Weinhold, F.; Carpenter, J. E. In *International Workshop on the Structure of Small Molecules and Ions*; Naaman, R., Vager, Z., Eds.; Plenum, New York, 1988].

Acknowledgments. We acknowledge with gratitude the contributions of many co-workers, as cited in the references. We thank John Carpenter and Eric Glen-dening for assistance with the figures and tables. This work was supported by the National Science Foundation, the Deutsche Forschungsgemeinschaft, and the Division of Materials Science, Office of Basic Energy Sciences, U.S. Department of Energy (Contract W-31-109-ENG-38).

References

- Dyke, T. R.; Howard, B. J.; Klemperer, W. *J. Chem. Phys.* 1972, 56, 2442-2454; Janda, K. C.; Steed, J. M.; Novick, S. E.; Klemperer, W. *J. Chem. Phys.* 1977, 67, 5162-5172; Klemperer, W. *Faraday Discuss. Chem. Soc.* 1977, 62, 179-184; Klemperer, W. *J. Mol. Struct.* 1980, 59, 161-176; Baiocchi, F. A.; Dixon, T. A.; Joyner, C. H.; Klemperer, W. *J. Chem. Phys.* 1981, 74, 6544-6549; Peterson, K. I.; Klemperer, W. *J. Chem. Phys.* 1984, 81, 3842-3845; Fraser, G. T.; Nelson, D. D.; Charo, A.; Klemperer, W. *J. Chem. Phys.* 1985, 82, 2535-2546; Nelson, D. D.; Fraser, G. T.; Klemperer, W. *Science* 1987, 238, 1670-1674.
- Dyke, T. R.; Mack, K. M.; Muenter, J. S. *J. Chem. Phys.* 1977, 66, 498-510; Odutola, J. A.; Dyke, T. R. *J. Chem. Phys.* 1980, 72, 5062-5070; Dyke, T. R. *Top. Curr. Chem.* 1984, 120, 85-113.
- Legon, A. C.; Soper, P. D.; Flygare, W. H. *J. Chem. Phys.* 1981, 74, 4944-4950; Soper, P. D.; Legon, A. C.; Read, W. G.; Flygare, W. H. *J. Chem. Phys.* 1982, 76, 292-300; Legon, A. C.; Millen, D. J. *Faraday Discuss. Chem. Soc.* 1982, 73, 71-87, 127-128, 128-129; Legon, A. C. *Annu. Rev. Phys. Chem.* 1983, 34, 275-300; Legon, A. C.; Millen, D. J. *Chem. Rev.* 1986, 86, 635-657; Legon, A. C.; Miller, D. *Acc. Chem. Res.* 1987, 20, 39-46.
- Fraser, G. T.; Pine, A. S. *J. Chem. Phys.* 1986, 85, 2502-2515; Lovejoy, C. M.; Schuder, M. D.; Nesbitt, D. J. *J. Chem. Phys.* 1986, 85, 4890-4902; Hwang, Z. S.; Jucks, K. W.; Miller, R. E. *J. Chem. Phys.* 1986, 85, 3338-3341.
- (a) Popkie, H.; Kistenmacher, H.; Clementi, E. *J. Chem. Phys.* 1973, 59, 1325-1336; Diercksen, G. H. F.; Kraemer, W. P.; Roos, B. O. *Theor. Chim. Acta* 1975, 36, 249-274; Mat-suoka, O.; Clementi, E.; Yoshimine, M. *J. Chem. Phys.* 1976, 64, 1351-1361; Newton, M. D.; Kestner, N. R. *Chem. Phys. Lett.* 1983, 94, 198-201; Frisch, M. J.; Pople, J. A.; Del Bene, J. E. *J. Chem. Phys.* 1983, 78, 4063-4065. (b) Schuster, P. In Schuster, P.; Zunel, G.; Sandorf, C., Eds. *The Hydrogen Bond*; North-Holland: New York, 1976; Vol. 1, pp 27-163.
- Ratajczak, H.; Orville-Thomas, W. J., Eds. *Molecular Interactions*; Wiley: Chichester, 1980; Vol. 1; van Duijneveldt-van der Rijdt, J. G. C. M.; van Duijneveldt, F. B. *Adv. Chem. Phys.* 1987, 69, 521; Hobza, P.; Zahradník, R. *Intermolecular Complexes*; Elsevier: Amsterdam, 1988; see also the "van der Waals Systems" issue of *Topics Curr. Chem.* 1980, 93.
- Foster, J. P.; Weinhold, F. *J. Am. Chem. Soc.* 1980, 102, 7211-7218. The INDO-SCF-MO implementation of the NBO procedure was incorporated in the BONDO program: Weinhold, F. *Quantum Chemistry Program Exchange No. 408*; Indiana University: Bloomington, IN, 1980. The ab initio implementation of this procedure was first formulated in terms of Löwdin orbitals (rather than NAOs): Rives, A. B.; Weinhold, F. *Int. J. Quantum Chem. Symp.* 1980, 14, 201-209; Weinstock, R. B. Ph.D. Thesis: University of Wisconsin: Madison, WI, 1981. In minimal basis sets these orbitals are similar, but as mentioned in section II.A, Löwdin OAOs must be replaced by NAOs in extended basis sets.
- Reed, A. E.; Weinhold, F. *J. Chem. Phys.* 1983, 78, 4066-4073.
- Reed, A. E.; Weinstock, R. B.; Weinhold, F. *J. Chem. Phys.* 1985, 83, 735-746.
- Löwdin, P.-O. *Phys. Rev.* 1955, 97, 1474-1489.
- (a) Pauling, L. *J. Am. Chem. Soc.* 1931, 53, 1367-1400; Slater, J. C. *Phys. Rev.* 1931, 37, 481-489; (b) Coulson, C. A. *Valence*, 2nd ed.; Oxford University Press: London, 1952.
- The formal mathematical necessity of including antibonds was apparently first noted by Dewar and Pettit (Dewar, M. J. S.; Pettit, R. *J. Chem. Soc.* 1954, 1625-1634) in the context of semiempirical Hückel-type theories. More general recognition of the key role of antibonds in many molecular phenomena was associated with development of the general LCBO-MO procedure for transforming SCF-MO wave functions to bond-orbital form: Weinhold, F.; Brunck, T. K. *J. Am. Chem. Soc.* 1976, 98, 3745-3749; Brunck, T. K.; Weinhold, F. *J. Am. Chem. Soc.* 1976, 98, 4392-4393; Brunck, T. K.; Weinhold, F. "Linear Combination of Bond Orbitals Approach to SCF-MO Theory", University of Wisconsin Theoretical Chemistry Institute Report WIS-TCI-560, 1976;

- cf. also ref 98. Natural bond orbitals may be considered to correspond to the particular form of the general bond-orbital transformation that minimizes the contribution of antibonds to the electron density (see ref 7).
- (13) For the general open-shell NBO procedure, leading to the concept of "different Lewis structures for different spins", see: Carpenter, J. E.; Weinhold, F. University of Wisconsin Theoretical Chemistry Institute Report WIS-TCI-689, 1985. See also ref 40, 84, and 85.
- (14) RHF: restricted Hartree-Fock. For an authoritative description of the standard ab initio computational methods and basis set designations referred to herein, see: Hehre, W. J.; Radom, L.; Schleyer, P. v. R.; Pople, J. A. *Ab Initio Molecular Orbital Theory*; Wiley: New York, 1986.
- (15) NBOs can be obtained for any wave function, correlated or uncorrelated. However, SCF-MO theory has generally been found adequate to describe qualitative trends in the structure and energetics of strongly bound van der Waals molecules, particularly those of H-bonded type (see, e.g., ref 6 and 14).
- (16) (a) Edmiston, C.; Ruedenberg, K. *Rev. Mod. Phys.* 1963, 34, 457-465. (b) Foster, J. M.; Boys, S. F. *Rev. Mod. Phys.* 1960, 32, 300-302; Boys, S. F. In Löwdin, P.-O., Ed. *Quantum Theory of Atoms, Molecules, and Solid State*; Academic: New York, 1966; p 253. (c) Weinstein, H.; Pauncz, R.; Cohen, M. *Adv. At. Mol. Phys.* 1971, 7, 97-140.
- (17) The general set of concepts developed by Klemperer and co-workers,¹² very similar in spirit to the NBO donor-acceptor picture presented here, is sometimes referred to as the "HOMO-LUMO model". Although this term is correctly suggestive of an association with occupied and unoccupied orbitals, we stress⁸ the essentially localized nature of these orbitals (though the distinction between BOs and MOs is blurred in the diatomic case) and the importance of spatial proximity ("overlap") of these orbitals, whether or not they are of "highest occupied" or "lowest unoccupied" type.
- (18) Mulliken, R. S. *J. Am. Chem. Soc.* 1952, 74, 811-824; *J. Phys. Chem.* 1952, 56, 801-822. Note, however, that the term "ionic resonance" was often synonymous (in resonance theory language) with interactions that, in MO theory, would be labeled as donor-acceptor type. Thus, Coulson's analysis (ref 11b, Chapter 13), leading to the conclusion that ionic resonance is the largest contribution to H-bonding in ice, is essentially consistent with the NBO donor-acceptor picture presented here.
- (19) Reed, A. E.; Weinhold, F. *QCPE Bull.* 1985, 5, 141.
- (20) (a) Binkley, J. S.; Frisch, M. J.; Defrees, D. J.; Raghavachari, K.; Whiteside, R. A.; Schlegel, H. B.; Fluder, E. M.; Pople, J. A. *GAUSSIAN-82*; Carnegie-Mellon University: Pittsburgh, 1984; see ref 14. The GAMESS program is originally due to: Dupuis, M.; Spangler, D.; Wendoloski, J. J. *NRCC Software Catalog*, Vol. 1; Program GG01, 1980. (c) MOPAC: Dewar, M. J. S.; Thiel, W. *J. Am. Chem. Soc.* 1977, 99, 4899; Dewar, M. J. S.; Stewart, J. J. P. *QCPE Bull.* 1985, 5, 455. (d) AMPAC: Dewar, M. J. S.; Stewart, J. J. P. *QCPE Bull.* 1986, 6, 506.
- (21) Pople, J. A.; Beveridge, D. L. *Approximate Molecular Orbital Theory*; McGraw-Hill: New York, 1970.
- (22) Löwdin, P.-O. *J. Chem. Phys.* 1950, 18, 365-375; Löwdin, P.-O. *Adv. Quantum Chem.* 1970, 5, 185-199.
- (23) Weinhold, F.; Carpenter, J. E. *J. Mol. Struct. (Theochem)*, 1988, 165, 189-202.
- (24) Jørgensen, P.; Simons, J. *J. Chem. Phys.* 1983, 79, 334-357.
- (25) See any elementary quantum mechanics text.
- (26) See, e.g.: Dewar, M. J. S.; Dougherty, R. C. *The PMO Theory of Organic Chemistry*; Plenum: New York, 1975; Burdett, J. K.; Hoffmann, R.; Fay, R. C. *Inorg. Chem.* 1978, 17, 2553-2568; Whangbo, M. H.; Schlegel, H. B.; Wolfe, S. *J. Am. Chem. Soc.* 1977, 99, 1296-1304.
- (27) Carlson, B. C.; Keller, J. M. *Phys. Rev.* 1957, 105, 102-103.
- (28) Mulliken, R. S. *J. Phys. Chem.* 1952, 56, 295-311.
- (29) Reed, A. E.; Schleyer, P. v. R. *J. Am. Chem. Soc.* 1987, 109, 7362-7373.
- (30) Mulliken, R. S. *J. Chem. Phys.* 1955, 23, 1833-1840, 1841-1846, 2338-2342, 2343-2346.
- (31) In addition to the works described elsewhere in this review, see, e.g.: Schleyer, P. v. R.; Pople, J. A. *Chem. Phys. Lett.* 1986, 129, 475-480; Bestmann, H. J.; Kos, A. J.; Witzgall, K.; Schleyer, P. v. R. *Chem. Ber.* 1986, 119, 1331-1349; Rajca, A.; Streitwieser, A.; Tolbert, L. M. *J. Am. Chem. Soc.* 1987, 109, 1790-1792; Kaufmann, E.; Schleyer, P. v. R.; Gronert, S.; Streitwieser, A.; Halpern, M. *J. Am. Chem. Soc.* 1987, 109, 2553-2559.
- (32) Carpenter, J. E.; Weinhold, F. *J. Am. Chem. Soc.* 1988, 110, 368-372.
- (33) Bent, H. A. *Chem. Rev.* 1961, 61, 275-311.
- (34) Reed, A. E.; Weinhold, F. *J. Chem. Phys.* 1985, 83, 1736-1740.
- (35) Nelsen, S. F.; Blackstock, S. C.; Yumibe, N. P.; Frigo, T. B.; Carpenter, J. E.; Weinhold, F. *J. Am. Chem. Soc.* 1985, 107, 143-149.
- (36) Reed, A. E.; Weinhold, F. *J. Am. Chem. Soc.* 1985, 107, 1919-1921.
- (37) Reed, A. E.; Weinhold, F. *J. Am. Chem. Soc.* 1986, 108, 3586-3593.
- (38) Reed, A. E.; Weinhold, F. *J. Chem. Phys.* 1986, 84, 2428-2430.
- (39) Carpenter, J. E.; Weinhold, F. *J. Phys. Chem.* 1986, 90, 6405-6408; Carpenter, J. E.; Weinhold, F. "Torsion-Vibration Interactions in Hydrogen Peroxide. I. Calculation of the Trans Barrier for OH Overtone Excitations up to $\nu = 8$. II. Natural Bond Orbital Analysis", University of Wisconsin Theoretical Chemistry Institute Report WIS-TCI-724, 1987; *J. Phys. Chem.*, in press.
- (40) Carpenter, J. E.; Weinhold, F. "Analysis of the Geometry of the Hydroxymethyl Radical by the Different Hybrids for Different Spins' Natural Bond Orbital Procedure", University of Wisconsin Theoretical Chemistry Institute Report WIS-TCI-718, 1987; *J. Mol. Struct. (Theochem)*, in press.
- (41) Reed, A. E. Ph.D. Thesis, University of Wisconsin, Madison, WI, 1985.
- (42) Horn, J. S.; Weinstock, R. B.; Weinhold, F. University of Wisconsin Theoretical Chemistry Institute Report WIS-TCI-604, 1979, unpublished.
- (43) Weinstock, R. B. Ph.D. Thesis, University of Wisconsin, Madison, WI, 1981.
- (44) Weinstock, R. B.; Weinhold, F. University of Wisconsin Theoretical Chemistry Institute Report WIS-TCI-661, 1981, unpublished.
- (45) Reed, A. E.; Weinhold, F.; Curtiss, L. A.; Pochatko, D. *J. Chem. Phys.* 1986, 84, 5687-5705.
- (46) Benzel, M. A.; Dykstra, C. E. *J. Chem. Phys.* 1983, 78, 4052-4062; 1984, 80, 3510-3511.
- (47) Benzel, M. A.; Dykstra, C. E. *Chem. Phys.* 1983, 80, 273-278.
- (48) Curtiss, L. A.; Pochatko, D. J.; Reed, A. E.; Weinhold, F. *J. Chem. Phys.* 1985, 82, 2679-2687.
- (49) Legon, A. C.; Soper, P. D.; Flygare, W. H. *J. Chem. Phys.* 1981, 74, 4944-4950.
- (50) (a) Spackman, M. A. *J. Chem. Phys.* 1986, 85, 6587-6601; (b) *J. Phys. Chem.* 1987, 91, 3179-3186.
- (51) The effects of steric repulsion were estimated from RHF/6-31G* calculations of He...OC and He...CO complexes. The interactions should be primarily of steric repulsion type. The small effects of charge transfer (primarily, from He 1s into σ^*_{CO}) were subtracted by the method of deletions to give the estimate $\Delta E_{EX} = \Delta E - \Delta E_{CT}$ of the steric terms. When He was placed at the respective distances (2.15 and 2.26 Å) of the H atom in CO...HF and OC...HF, the values of ΔE_{EX} (3.82 and 7.56 kcal/mol) suggest a steric difference of at least 3-4 kcal/mol favoring the wrong isomer. (See ref 45 for more details.)
- (52) Rensberger, K. J.; Blair, J. T.; Weinhold, F.; Crim, F. F. "Experimental and Theoretical Study of the Relaxation of vibrationally excited HF by NO and CO", University of Wisconsin Theoretical Chemistry Institute Report WIS-TCI-732, 1987.
- (53) Copeland, R. A.; Pearson, D. J.; Robinson, J. M.; Crim, F. F. *J. Chem. Phys.* 1982, 77, 3974-3982; 1983, 78, 6344; Robinson, J. M.; Rensberger, K. J.; Crim, F. F. *J. Chem. Phys.* 1986, 84, 220-226.
- (54) Del Bene, J.; Pople, J. A. *J. Chem. Phys.* 1970, 52, 4858-4866.
- (55) Kollman, P. A.; Allen, L. C. *Chem. Rev.* 1972, 72, 283-303.
- (56) Tanford, C. *The Hydrophobic Effect: Formation of Micelles and Biological Membranes*, 2nd ed.; Wiley: New York, 1980; Ben-Naim, A. *Hydrophobic Interactions*; Plenum: New York, 1980. For some of the controversy surrounding this subject, see, e.g.: Hildebrand, J. H. *J. Phys. Chem.* 1968, 72, 1841-1842; *Proc. Natl. Acad. Sci. U.S.A.* 1979, 76, 194; Némethy, G.; Scheraga, H. A.; Kauzmann, W. *J. Phys. Chem.* 1968, 72, 1842; Tanford, C. *Proc. Natl. Acad. Sci. U.S.A.* 1979, 76, 4175-4176.
- (57) See, e.g.: Kauzmann, W. *Adv. Protein Chem.* 1959, 14, 1-63; Edsall, J. T.; McKenzie, H. A. *Adv. Biophys.* 1978, 10, 137-207; 1983, 16, 53-183; Saenger, W.; Hunter, W. N.; Kennard, O. *Nature (London)* 1986, 324, 385-388.
- (58) Hvidt, A. *Annu. Rev. Biophys. Bioeng.* 1983, 12, 1-20.
- (59) Ungemach, S. R.; Schaefer, H. F. *J. Am. Chem. Soc.* 1974, 96, 7898-7901.
- (60) Kollman, P.; McKelvey, J.; Johansson, A.; Rothenberg, S. J. *J. Am. Chem. Soc.* 1975, 97, 955-965; Swaminathan, S.; Harrison, S. W.; Beveridge, D. L. *J. Am. Chem. Soc.* 1978, 100, 5705-5712.
- (61) Seiler, P.; Weisman, G. R.; Glendening, E. D.; Weinhold, F.; Johnson, V. B.; Dunitz, J. D. "Observation of an Eclipsed C(sp³)-CH₃ Bond in a Tricyclic Orthoamide: Experimental and Theoretical Evidence for C-H...O Hydrogen Bonds", University of Wisconsin Theoretical Chemistry Institute Report WIS-TCI-710, 1987; *Angew. Chem.* 1987, 99, 1216-1218; *Angew. Chem., Int. Ed. Engl.* 1987, 26, 1175-1177.
- (62) Even this value is misleading, since the 6-31G* basis set (cf. also ref 59) significantly overestimates the SCF value of the C-H...O bond strength. In basis sets including adequate diffuse functions (e.g., 6-31++G* or TZP), the SCF contribution is reduced to about 0.1 kcal/mol, while the correlation

- correction is little affected. Thus, the correlation "correction" may be 5–10 times the SCF result in larger basis sets!
- (63) Schuster, P.; Zundel, G.; Sandorfy, C., Eds. *The Hydrogen Bond*; North-Holland: Amsterdam, 1976; Amos, R. D. *Chem. Phys.* 1986, 104, 145–151.
- (64) (a) Zilles, B. A.; Person, W. B. *J. Chem. Phys.* 1983, 79, 65–77. (b) Swanton, D. J.; Bacsikay, G. B.; Hush, N. S. *Chem. Phys.* 1983, 82, 303–315.
- (65) Castiglioni, C.; Gussoni, M.; Zerbi, G. *J. Chem. Phys.* 1984, 80, 3916–3918.
- (66) (a) Huyskens, P. L. *J. Am. Chem. Soc.* 1977, 99, 2578–2582. (b) Kleeberg, H.; Klein, D.; Luck, W. A. P. *J. Phys. Chem.* 1987, 91, 3200–3203; Curtiss, L. A.; Blander, M. *Chem. Rev.*, this issue.
- (67) Peterson, K. I.; Klemperer, W. *J. Chem. Phys.* 1984, 80, 2439–2445.
- (68) Fraser, G. T.; Leopold, K. R.; Klemperer, W. *J. Chem. Phys.* 1984, 81, 2577–2584; Fraser, G. T.; Nelson, D. D., Jr.; Gerfen, G. J.; Klemperer, W. *J. Chem. Phys.* 1985, 83, 5442–5449; Peterson, K. I.; Klemperer, W. *J. Chem. Phys.* 1986, 85, 725–732.
- (69) See, e.g.: Malm, J. G.; Selig, H.; Jortner, J.; Rice, S. A. *Chem. Rev.* 1965, 65, 199–236.
- (70) See, e.g.: Sharfin, W.; Johnson, K. E.; Wharton, L.; Levy, D. H. *J. Chem. Phys.* 1979, 71, 1292–1299; Levy, D. H. *Adv. Chem. Phys.* 1981, 47, 323–363; Mills, P. D. A.; Western, C. M.; Howard, B. J. *J. Chem. Phys.* 1986, 90, 4961–4969; Lonszczy, M.; Moscowitz, J. W.; Stillinger, F. H. *J. Chem. Phys.* 1974, 61, 2438–2441; Fowler, P. W.; Buckingham, A. D. *Mol. Phys.* 1983, 50, 1349–1361.
- (71) Koch, W.; Collins, J. R.; Frenking, G. *Chem. Phys. Lett.* 1986, 132, 330–333; Koch, W.; Frenking, G. *Int. J. Mass Spectrom. Ion Proc.* 1986, 74, 133. Koch, W.; Frenking, G.; Gauss, J.; Cremer, D.; Collins, J. R. *J. Am. Chem. Soc.* 1987, 109, 5917–5934.
- (72) Hobza, P.; Schleyer, P. v. R., *Coll. Czech. Chem. Comm.*, in press.
- (73) Kebarle, P. *Annu. Rev. Phys. Chem.* 1977, 28, 445–476.
- (74) Karpfen, A.; Schuster, P. In Dogonadze, R.; Kalman, E.; Kornyshev, A. A.; Ulstrup, J., Eds. *The Chemical Physics of Solvation, Part A*; Elsevier: Amsterdam, 1985; p 265.
- (75) Curtiss, L. A.; Melendres, C. A.; Reed, A. E.; Weinhold, F. J. *Comput. Chem.* 1986, 1, 294–305.
- (76) (a) Jafri, J. A.; Logan, J.; Newton, M. D. *Isr. J. Chem.* 1980, 19, 340–350. (b) Curtiss, L. A.; Halley, J. W.; Hautman, J.; Rahman, A. J. *Chem. Phys.* 1987, 86, 2319–2327. (c) Newton, M. D. *Acta Crystallogr., Sect. B* 1983, 39, 104–113; *J. Phys. Chem.* 1983, 87, 4288–4292; Tse, Y.-C.; Newton, M. D. *J. Am. Chem. Soc.* 1977, 99, 611–612; Yoon, B. J.; Morokuma, K.; Davidson, E. R. *J. Chem. Phys.* 1985, 83, 1223–1231; Morse, M. D.; Rice, S. A. *J. Chem. Phys.* 1982, 76, 650–660; Townsend, M.; Rice, S. A.; Morse, M. D. *J. Chem. Phys.* 1983, 79, 2496–2498; Nielson, G.; Rice, S. A. *J. Chem. Phys.* 1984, 80, 4456–4463.
- (77) Almlöf, J. *Chem. Phys. Lett.* 1972, 17, 49–52.
- (78) Pimentel, G. C. *J. Chem. Phys.* 1951, 19, 446–448.
- (79) Weiss, R.; Wolf, H.; Schubert, U.; Clark, T. *J. Am. Chem. Soc.* 1981, 103, 6142–6147; Weiss, R.; Reinhardt, W., unpublished.
- (80) Bühl, R. E.; Hurni, B. *Helv. Chim. Acta* 1978, 61, 90–96.
- (81) Reed, A. E.; Weinhold, F.; Weiss, R.; Macheleid, J. *J. Phys. Chem.* 1985, 89, 2688–2694. Extension of these calculations by Reed (Reed, A. E., unpublished) to the MP2FU/6-31G* geometry optimization level confirms these results, and the $\text{Cl}_2\text{C}^+ \cdots \text{Cl}^-$ complex is found to be 19.2 kcal mol⁻¹ lower in energy than isolated $\text{CCl}_2 + \text{Cl}_2$. The Cl–Cl distance decreased to 2.50 Å in the complex; other parameters changed little.
- (82) Ostrander, S. C.; Sanders, L. A.; Weisshaar, J. C. *J. Chem. Phys.* 1986, 84, 529–530.
- (83) Flamme, J. P.; Mark, T.; Los, J. *Chem. Phys. Lett.* 1980, 75, 419–422; Moseley, J. T.; Saxon, R. P.; Huber, B. A.; Cosby, P. C.; Abouaf, R.; Tadjeddine, M. *J. Chem. Phys.* 1977, 67, 1659–1668; Abouaf, R.; Huber, B. A.; Cosby, P. C.; Saxon, R. P.; Moseley, J. T. *J. Chem. Phys.* 1978, 68, 2406–2410; Vanderhoff, J. A. *J. Chem. Phys.* 1977, 67, 2332–2337; Smith, G. P.; Cosby, P. C.; Moseley, J. T. *J. Chem. Phys.* 1977, 67, 3818–3828; Smith, G. P.; Lee, L. C. *J. Chem. Phys.* 1979, 69, 5393–5399; Ostrander, S. C.; Weisshaar, J. C. *Chem. Phys. Lett.* 1986, 129, 220–224.
- (84) Blair, J. T.; Weisshaar, J. C.; Carpenter, J. E.; Weinhold, F. *J. Chem. Phys.* 1987, 87, 392–410.
- (85) Blair, J. T.; Weisshaar, J. C.; Weinhold, F. *J. Chem. Phys.*, 1988, 88, 1467–1468.
- (86) Cotton, F. A.; Wilkinson, G. *Advanced Inorganic Chemistry*, 3rd ed.; Wiley: New York, 1972.
- (87) Albright, T. A.; Burdett, J. K.; Whangbo, M.-H. *Orbital Interactions in Chemistry*; Wiley: New York, 1985.
- (88) Sung, S.-S.; Hoffmann, R. *J. Am. Chem. Soc.* 1985, 107, 578–584.
- (89) Post, D.; Baerends, E. J. *Surf. Sci.* 1982, 116, 177–187.
- (90) March, N. H. *Chemical Bonds Outside Metal Surfaces*; Plenum: New York, 1986.
- (91) Reed, A. E.; Curtiss, L. A.; Weinhold, F., in preparation.
- (92) (a) Bagus, P. S.; Nelin, C. J.; Bauschlicher, C. W. *Phys. Rev.* 1983, B28, 5423–5438. (b) Bagus, P. S.; Hermann, K.; Bauschlicher, C. W. *J. Chem. Phys.* 1984, 80, 4378–4386. (c) Hermann, K.; Bagus, P. S.; Bauschlicher, C. W. *Phys. Rev.* 1984, B30, 7313–7316; Bagus, P. S.; Hermann, K. *Phys. Rev.* 1986, B33, 2987–2991.
- (93) Cf. also: Bagus, P. S.; Hermann, K.; Müller, W.; Nelin, C. J. *Phys. Rev. Lett.* 1986, 57, 1496; Bagus, P. S.; Nelin, C. J.; Müller, W.; Philpott, M. R.; Seki, H. *Phys. Rev. Lett.* 1987, 58, 559–562; Wimmer, E.; Fu, C. L.; Freeman, A. L. *Phys. Rev. Lett.* 1985, 55, 2618–2621; 1986, 57, 1497.
- (94) Bauschlicher, C. W. *Chem. Phys.* 1986, 106, 391–398.
- (95) Kitaura, K.; Morokuma, K. *Int. J. Quantum Chem.* 1976, 10, 325–340.
- (96) Umeyama, H.; Morokuma, K. *J. Am. Chem. Soc.* 1977, 99, 1316–1332.
- (97) Tatar, R. C.; Messmer, R. P. *J. Vac. Sci. Technol. A* 1987, 5, 675–678.
- (98) Brunck, T. K.; Weinhold, F. *J. Am. Chem. Soc.* 1979, 101, 1700–1709.
- (99) Corcoran, C. T.; Weinhold, F. *J. Chem. Phys.* 1980, 72, 2866–2868.
- (100) Cf. also: Tyrrell, J.; Weinstock, R. B.; Weinhold, F. *Int. J. Quantum Chem.* 1981, 19, 781–791; Wesenberg, G.; Weinhold, F. *Int. J. Quantum Chem.* 1982, 21, 487–509; ref 39 and 40.
- (101) See, e.g.: Schleyer, P. v. R.; Kos, A. J. *Tetrahedron* 1983, 39, 1141–1150 and references therein.
- (102) The major comprehensive reviews of this field are the following: (a) Kirby, A. J. *The Anomeric Effect and Related Stereoelectronic Effects at Oxygen*; Springer: Berlin, 1983. (b) Deslongchamps, P. *Stereoelectronic Effects in Organic Chemistry*; Pergamon: New York, 1983. (c) Gorenstein, D. G. *Chem. Rev.* 1987, 87, 1047–1077.
- (103) (a) Reference 29. (b) Reed, A. E.; Schleyer, P. v. R. *Inorg. Chem.*, in press. (c) Reed, A. E.; Schade, C.; Schleyer, P. v. R.; Kamath, P. V.; Chandrasekhar, J. *J. Chem. Soc., Chem. Commun.* 1988, 67–69. (d) Reed, A. E.; Schleyer, P. v. R., in preparation.
- (104) See, e.g.: Désilets, S.; St.-Jacques, M. *J. Am. Chem. Soc.* 1987, 109, 1641–1648; Fuch, P.; Ellencweig, A.; Tartakovsky, E.; Aped, P. *Angew. Chem.* 1986, 98, 289–290.
- (105) See, e.g.: Wong, J. S.; Moore, C. B. *J. Chem. Phys.* 1982, 77, 603–615 and references therein.
- (106) Stretching the bond lowers the antibond energy, making it a better acceptor. In the limiting case the antibond orbital becomes an isolated radical orbital, providing an orbital vacancy deep in the valence shell rather than a high-energy antibond.
- (107) Döhla, H.-R.; Crim, F. F. *J. Chem. Phys.* 1985, 83, 3863–3872.
- (108) Lovejoy, C. M.; Nesbitt, D. J. *J. Chem. Phys.* 1987, 86, 3151–3165, and references therein.
- (109) The term "van der Waals force" has often been equated with the London dispersion force. This designation is improper,¹¹⁰ however, for dispersion forces have a leading dependence on the intermolecular distance of R^{-7} . In contrast, the intermolecular forces implicit in the van der Waals equation of state¹¹¹ have an R^{-4} dependence,¹¹⁰ as may be seen by extension of the discussion in: Moore, W. J. *Physical Chemistry*, 4th ed.; Prentice-Hall: New York, 1972; pp 126–127.
- (110) Moelwyn-Hughes, E. A. *Physikalische Chemie*; Thieme: Stuttgart, 1970.
- (111) van der Waals, J. D., Sr. "Die Kontinuität des gasförmigen und flüssigen Zustands", Dissertation, Leiden, 1873.
- (112) Lewis, G. N. *Valence and the Structure of Atoms and Molecules*; The Chemical Catalog Co.: New York, 1923.
- (113) Huggins, M. L. Thesis, University of California, 1919; Latimer, W. M.; Rodebush, W. H. *J. Am. Chem. Soc.* 1920, 42, 1419–1433.
- (114) Pauling, L. *Proc. Natl. Acad. Sci. U.S.A.* 1928, 14, 359–362; *J. Am. Chem. Soc.* 1931, 53, 1367–1400.
- (115) Pimentel, G. C.; McClellan, A. L. *The Hydrogen Bond*; W. H. Freeman: San Francisco, 1960. As these authors point out (pp 244–245), an electrostatic model with sufficient parameters could logically be extended to give an analogous "point charge model" of covalent bonding!
- (116) Pimentel, G. C.; McClellan, A. L. *Annu. Rev. Phys. Chem.* 1971, 22, 347–381; cf. also: Bratoz, S. *Adv. Quantum Chem.* 1967, 3, 209–239.
- (117) Coulson, C. A. *Research* 1957, 10, 149–159. The largest contribution to H-bond attraction is found to be the "delocalization" term (labeled "ionic resonance" in ref 11b; cf. ref 18). Of the smaller electrostatic contributions, Coulson writes, "It is tempting to argue that in view of the close agreement between this electrostatic energy and the hydrogen bond energy, a true account has been obtained of the most important factors involved. But this is not so."

- (118) (a) Kollman, P. A. *J. Am. Chem. Soc.* 1977, 99, 4875–4894.
 (b) Singh, U. C.; Kollman, P. *J. Chem. Phys.* 1984, 80, 353–355.
- (119) Morokuma, K. *Acc. Chem. Res.* 1977, 10, 294–300.
- (120) Cf. also ref 46, 47, 50, and 65; Michael, D. W.; Dykstra, C. E.; Lisy, J. M. *J. Chem. Phys.* 1984, 81, 5998–6006; Liu, S.-Y.; Michael, D. W.; Dykstra, C. E.; Lisy, J. M. *J. Chem. Phys.* 1986, 84, 5032–5036; Liu, S.-Y.; Dykstra, C. E.; Kohenbrander, K.; Lisy, J. M. *J. Chem. Phys.* 1986, 85, 2077–2083; Dykstra, C. E.; Liu, S.-Y.; Malik, D. J. *J. Mol. Struct. (Theochem)* 1986, 135, 357–368; Rendell, A. P. L.; Bacskay, G. B.; Hush, N. S. *Chem. Phys. Lett.* 1985, 117, 400–408; Hurst, G. B.; Fowler, P. W.; Stone, A. J.; Buckingham, A. D. *Int. J. Quantum. Chem.* 1986, 29, 1223–1239.
- (121) (a) Some recent examples are: Hall, D.; Pavitt, N. *J. Comput. Chem.* 1984, 5, 441–450; Kim, K. S.; Clementi, E. *J. Am. Chem. Soc.* 1985, 107, 5504–5513; Nilsson, L.; Karplus, M. *J. Comput. Chem.* 1986, 7, 591–616; Weiner, S. J.; Kollman, P. A.; Nguyen, D. T.; Case, D. A. *J. Comput. Chem.* 1986, 7, 230–252; Heinzinger, K.; Palinkas, G., in ref 74, pp 313–353.
 (b) For application reviews, see, e.g.: Fröhbeis, H.; Klein, R.; Wallmeier, H. *Angew. Chem.* 1987, 99, 413–428; Sheridan, R. P.; Venkataraman, R. *Acc. Chem. Res.* 1987, 20, 322–329.
- (122) Buckingham, A. D.; Fowler, P. W. *J. Chem. Phys.* 1983, 79, 6426–6428; Buckingham, A. D.; Fowler, P. W. *Can. J. Chem.* 1985, 63, 2018–2025; Buckingham, A. D. *Chem. Rev.*, this issue.
- (123) Baiocchi, F.; Reiher, W.; Klemperer, W. *J. Chem. Phys.* 1983, 79, 6428–6429.
- (124) Stevens, W. J.; Fink, W. H. *Chem. Phys. Lett.* 1987, 139, 15–22.
- (125) Smits, G. F. Ph.D. Thesis, University of Leiden, 1985; Smits, G. F.; Altona, C. *Theor. Chim. Acta* 1985, 67, 461–475; Smits, G. F.; Krol, M. C.; van der Hart, W. J.; Altona, C. *Mol. Phys.* 1986, 59, 209–255.
- (126) Morokuma, K.; Umeyama, H. *Chem. Phys. Lett.* 1977, 49, 333–337.
- (127) Sovers, O. J.; Kern, C. W.; Pitzer, R. M.; Karplus, M. *J. Chem. Phys.* 1968, 49, 2592–2599.
- (128) In this case, classical electrostatic energy favors the eclipsed conformation,^{125–127} consistent with the Pauli exclusion violating $\sigma_{\text{CH}} \rightarrow \sigma_{\text{CH}}^*$ interaction that is maximized in the eclipsed conformation. The Morokuma-type analysis methods incorporate the $\sigma_{\text{CH}} \rightarrow \sigma_{\text{CH}}^*$ stabilization into the electrostatic term ΔE_{ES} , and this partially cancels the $\sigma_{\text{CH}} \rightarrow \sigma_{\text{CH}}^*$ term that is also a part of the ΔE_{ES} term, since these two interactions have opposite dependencies on the HCCCH dihedral angle. The rotation barrier then appears to be due to exclusion repulsion between vicinal σ_{CH} orbitals.¹²⁷ This exclusion repulsion term is primarily correcting for the Pauli-principle-violating contributions to the electrostatic energy. See ref 23 and 99 for additional discussion of the role of nonorthogonality in rotation barrier analysis.
- (129) (a) Weiner, P.; Kollman, P. *J. Comput. Chem.* 1981, 2, 287–303. (b) Karplus, M.; McCammon, J. A. *Annu. Rev. Biochem.* 1983, 52, 263–300; Nemethy, G.; Pottle, M. S.; Scheraga, H. A. *J. Phys. Chem.* 1983, 87, 1883–1887.
- (130) See, e.g., ref 121a, 129a, and: Weiner, S. J.; Kollman, P. A.; Case, D. A.; Singh, U. C.; Ghio, C.; Alagona, G.; Profeta, S., Jr.; Weiner, P. *J. Am. Chem. Soc.* 1984, 106, 765–784.
- (131) Dr. K. Müller (Hoffmann-La Roche, Basel), lecture at DFG Schwerpunkt meeting in Heidelberg, April 1987.
- (132) For example, Umeyama and Morokuma⁹⁸ conclude that “[charge transfer] plays a relatively minor role in a strong, more ES [electrostatic] hydrogen bond such as N…HF” and Benzel and Dykstra⁴⁶ find “no evidence of any meaningful extent of charge transfer” in the OC…HF complex. Cf. also ref 55.
- (133) See, e.g.: Hirschfelder, J. O.; Curtiss, C. F.; Bird, R. B. *Molecular Theory of Gases and Liquids*; Wiley: New York, 1954; p 955ff.
- (134) Pauling, L. *The Nature of the Chemical Bond*; Cornell University Press: Ithaca, NY, 1960; p 263.
- (135) Gibbs, J. W. (letter of acceptance of the Rumford Medal, Jan 10, 1881); quoted in Wheeler, L. P. *Josiah Willard Gibbs, The History of a Great Mind*; Yale University Press: New Haven, CT, 1962; p 88.
- (136) See, e.g.: Bent, H. A. *Chem. Rev.* 1968, 68, 587–648; Clark, T. *J. Am. Chem. Soc.* 1987, 109, 1013–1020; Record, M. T.; Richey, B. *Physical Chemical Analysis of Biopolymer Self-Assembly Interactions*; American Chemical Society Sourcebook, in press. For host-guest and biological recognition interactions, see, e.g. Volumes 98, 101, 114, 121, 128, 132, 136, and 140 of *Topics in Current Chemistry*; Lehn, J. M. *Angew. Chem.* 1988, 100, 91–116.
- (137) Newton, M. D. *Trans. Am. Crystallogr. Assoc.* 1986, 22, 1–22.